

# BETA PICTORIS: An Early Solar System?

*Pawel Artymowicz*

Stockholm Observatory, Stockholm University, S-133 36 Saltsjöbaden, Sweden, and  
Space Telescope Science Institute, 3700 San Martin Drive, Baltimore, Maryland  
21218; e-mail: pawel@astro.su.se

KEY WORDS: Beta Pictoris, circumstellar dust disks, planetesimals; planetary systems: formation, extrasolar, solar

---

## ABSTRACT

Beta Pictoris ( $\beta$  Pic) is the best studied of the normal main-sequence stars surrounded by circumstellar dust disks. We review the status of  $\beta$  Pic and its disk, and compare it with both the early and the present Solar System. The disk has very little gas and therefore is more evolved and older than the primordial solar nebulae, which persist for 1–10 Myr. We concentrate on the observed optical properties, spatial and size distribution, mineralogy, and physics of the dust component, all of which are similar, if not identical, to those of the interplanetary and cometary dust in the Solar System. The most important process in the disk is collisional fragmentation of orbiting solid bodies, leading to the eventual removal of micron-sized and smaller debris from the system by radiation pressure. Silicate dust and sand, as well as planetesimals (perhaps comets) are observed around the star in quantities that are orders of magnitude larger than those in the present Solar System, but are consistent with a young solar system in the clearing stage. Theory of the  $\beta$  Pic disk indicates that its age must be  $\lesssim 100$  Myr, and its mass comparable with that of all solid bodies in our system. Several indirect arguments support the hypothetical existence of planet(s) in orbit around the star. Our current knowledge strongly suggests a positive answer to the title question.

---

## 1. INTRODUCTION

The search for and discovery of extrasolar planetary systems proceed at a rapid pace. First, two Earth-mass planets (and now the third smaller one) orbiting around pulsar PSR 1257+12 were serendipitously found (Wolszczan & Frail 1992, Wolszczan 1994). Then Mayor & Queloz (1995) found a Jupiter-mass

companion to the star 51 Pegasi, circling the sun-like star at a distance of  $a = 0.05$  AU, one hundredth of the distance between Jupiter and the Sun. Just months later, Jovian and super-Jovian mass companions were announced by Marcy & Butler (1996a) around 70 Virginis ( $a = 0.43$  AU), Butler & Marcy (1996) around 47 Ursae Majoris ( $a = 2.1$  AU), and very recently 55  $\rho^1$  Cancri ( $a = 0.11$  AU),  $\tau$  Boötis ( $a = 0.05$  AU), and  $\nu$  Andromedae ( $a = 0.06$  AU) (Marcy & Butler 1996b). A low-mass companion to star HD114762 may also be a planet with  $a = 0.3$  AU (Latham et al 1992). Assuming that all of these extrasolar companions are indeed planets, we now know of more planets outside than inside our Solar System. From available statistics, at least about 5% of the stars similar to the Sun may have giant planets. Many of the remaining stars may have long-period planets and/or currently undetectable, Earth-like planets.

The existence of a theoretically surmised but heretofore unseen trans-Neptunian part of our Solar System was confirmed by observations (Jewitt & Luu 1993, review by Weissman 1995). A disk of comets/icy asteroids, also known as the Kuiper belt, contains tens of thousands of sizable bodies ( $\gtrsim 100$ -km diameter) and  $\sim 10^9$  small comets, and extends between 40 AU and  $\sim 10^3$  AU from the Sun.

These new developments are giving a new perspective to our knowledge of a dusty circumstellar disk around Beta Pictoris ( $\beta$  Pic), a nearby and seemingly normal main sequence star hotter and more massive than the Sun (spectral type A5V). For more than a decade, this system has been under intense scrutiny because of its suspected similarity to either a forming or a young planetary system. With the growing realization that planetary systems are not uncommon, we are more than ever motivated to tackle questions such as how similar is the dust around  $\beta$  Pic to the solar system dust? Is there evidence for the existence of large bodies (comets, asteroids, Earth-like planets, giant planets)? Are we observing an extrasolar Kuiper disk? Due to what physical processes and how fast is the system evolving? Is it an early Solar System?

Beta Pictoris first jumped from obscurity to headlines in 1983 when the Infrared Astronomical Satellite (IRAS) serendipitously discovered a class of Vega-type systems. These systems (named after the prototype star Vega, or  $\alpha$  Lyr) emit a large flux of infrared (IR) radiation, much in excess of what their stellar photospheres can supply.  $\beta$  Pic is the most prominent member of that class. It is also by far the best studied Vega-type star owing in no small measure to coronagraphic imaging of its edge-on dusty circumstellar disk, pioneered by Smith & Terrile (1984). The telltale IR excess was shown to be the thermal radiation from solid grains with sizes larger than  $1 \mu\text{m}$ , i.e. very much larger than typically found in the interstellar medium (hereafter ISM), heated by the star to a temperature  $T \sim 100$  K. The grains are in orbit around  $\beta$  Pic and

other host stars. We now believe that many normal main-sequence stars, both Sun-like ( $\geq 50\%$  of G-type stars) and somewhat more massive stars (10–50% of type B, A, or F stars) are surrounded by cold dust disks (Aumann 1988, Aumann & Good 1990, Backman & Paresce 1993). Our Sun also supports a tenuous disk of dust, the zodiacal light disk covering the whole planetary region and probably joining a dusty component of the Kuiper belt further out (Good et al 1986, Gustafson 1994). The early Solar System, up to about 600–800 Myr (Myr = million years) after formation, contained much more solid debris than now, ranging in size from dust and meteoroids to planetesimals (geologically undifferentiated, planet-building cometary/asteroidal bodies  $> 1$  km in size) and protoplanets.

The ages of individual Vega-type stars span their whole main-sequence lifetime. We are thus not merely witnessing the “excesses of the youth,” phenomena found only in Young Stellar Objects and the pre-main sequence stars, lasting for a few million years (denoted Myr hereafter). While there is a growing consensus that the Vega phenomenon derives from the common occurrence of planetary systems around stars, we do not know in general whether we are dealing with forming, already formed, or “failed” planetary systems. Some disks surrounding Vega-type stars may constitute “missing links” between pre-main sequence objects (T Tauri, Herbig Ae/Be stars) and the finished solar-like systems (where the solid material is almost exclusively in the planets, and relatively little dust is present). Others may remain dusty but without planets forever.

$\beta$  Pic can be seen with the naked eye in the southern sky from locations south of and including Hawaii. Enough detailed astronomical data on  $\beta$  Pic, (obtained by a wide array of instruments) exist now to make  $\beta$  Pic resemble the proverbial elephant being studied by blindfolded persons, each pronouncing a somewhat different truth about the nature of the elephant. A single review can no longer do justice to every important aspect of the system. We approach the subject from the side of the dominant dusty “body,” and study its “physiology” and age, as well as the hypothetical existence of planet(s). Other recent reviews partly devoted to  $\beta$  Pic were written by Norm & Paresce (1989), Backman & Paresce (1993), Sicardy (1993), and Lagrange (1995). Many recommended reviews and contributions are collected in Ferlet & Vidal-Madjar (1994).

## 2. FORMING SOLAR SYSTEMS

The theory and astronomical observations related to the formation of solar systems provide a natural framework for describing and understanding the phenomena we find in  $\beta$  Pic. Thorough reviews of planetary system formation can be found in Weaver & Danly (1989), Wetherill (1990), Levy et al (1993), and Lissauer (1993). Below we briefly discuss issues particularly relevant to  $\beta$  Pic.

## 2.1 *Solar Nebulae*

Planetary systems form from dusty gaseous protoplanetary disks with typical radii of 100 AU (observed range:  $10\text{--}10^3$  AU), containing a cosmic (=solar) abundance of 2% by mass of heavy elements relative to H and He. Protoplanetary disks are essentially identical with optically thick, protostellar/circumstellar accretion disks that are observed to surround from 50–90% of the youngest pre-main sequence objects in star-forming regions. A gas disk is also a necessary component in every modern theory of star formation. Thus  $\beta$  Pic had a good a priori chance to exhibit at birth a Laplacean protoplanetary disk referred to as a solar nebula. A nebula with a particular surface density distribution decreasing as  $\Sigma(r) \sim r^{-3/2}$  with radius  $r$ , and just enough mass of refractory elements to form (with 100% efficiency) all Solar System planets and comets, is called the minimum solar nebula. Its mass is equal to<sup>1</sup>  $0.02 M_{\odot}$  (or only  $0.013 M_{\odot}$ , disregarding a massive Oort cloud of comets extending to  $\sim 10^5$  AU from the Sun). The actual mass of the primordial disk in our system must have been several times the above minimum (Lissauer 1993); most likely it was  $0.05$  to  $0.1 M_{\odot}$ . A similar mass might have been present in the pre-main sequence disk of  $\beta$  Pic, a star 1.7 times more massive than the Sun. Observationally, disk masses range from  $0.01$  to  $0.1 M_{\odot}$ , and their survival time as massive optically thick structures around solar-type stars equals  $\sim 3$  to  $10$  Myr. The shorter of the two times applies to  $\beta$  Pic as an intermediate-mass star (Strom et al 1993). After that time, photoevaporation and other processes are believed to remove the bulk of gas and fine dust.

## 2.2 *Mineralogy and Ice/Dust Ratio of Solids*

Very early, perhaps only  $10^4$  year after solar nebula formation, solid objects larger than  $\sim 1$  cm accumulate in the course of low-velocity collisions and gather on circular orbits near the equatorial plane of the disk, where they grow further to the size of planetesimals (1 km or more). Their composition is, broadly speaking, chondritic. Most C and O remain as gaseous CO in the disk, while the “unused” O binds with the abundant Si, Mg, and Fe (as well as less abundant refractory elements) in silicate grains. Chemical condensation models predict this happens in the cooling (inner) nebula as the gas temperature falls below  $T \sim 1400\text{--}1700$  K. Forsterite  $\text{Mg}_2\text{SiO}_4$  and enstatite  $\text{MgSiO}_3$  are the most important abundant silicate minerals above  $T \sim 500$  K (Wood & Hashimoto 1993). Ca, Al, and Na-containing silicates diopside and albite contribute  $<20\%$  to the condensed mass. Below 500 K (unless kinetically prohibited) Fe, first condensed in separate Fe and FeS grains, oxidizes and

<sup>1</sup>In the following, we often denote one solar mass as  $M_{\odot}$ , and one Earth mass as  $M_E = 3 \times 10^{-6} M_{\odot}$ .

becomes incorporated into the silicate solid solutions of olivines ( $\text{Mg, Fe})_2\text{SiO}_4$ , and pyroxenes ( $\text{Mg, Fe})\text{SiO}_3$ , with a typical  $\text{Fe}:(\text{Fe} + \text{Mg})$  mass ratio equal 1:5. In the cold outer part of the nebula this simple condensation sequence is complicated by the preservation of interstellar silicates and ices ( $\sim 90\%$   $\text{H}_2\text{O}$ , plus  $\text{CO}_2$  and  $\text{CO}$ ,  $\text{NH}_3$ ,  $\text{CH}_4$ ,  $\text{N}_2$  ices may have been incorporated in comets at  $r \gtrsim 20$  AU). Only one third to one half of the mass of an “icy” body formed in the standard nebula is ice—this percentage was found in comets, Pluto/Charon, some outer solar system satellites, as well as in cosmochemical theory (McDonnell et al 1991, Skyes & Walker 1992, Prinn 1993).

### 2.3 *The Total Mass of Solid Planetesimals*

Based on the above discussion and the cosmic elemental abundances, both in our system and in the protostellar disk surrounding  $\beta$  Pic for the first few Myr, we expect that a total condensible fraction equal to 0.5% of the total gas mass, or  $(0.5\%) \times (0.05 - 0.1)M_\odot \sim (120 \pm 40)M_E$ , may have been available for the formation of silicate and icy planetesimals including some CHON organic component.

### 2.4 *Runaway Accumulation of Protoplanets in our System*

In the solar system, binary collisions and accumulation rearranged an orbitally unstable set of  $\sim 10^{14}$ -km-sized planetesimals into the set of  $\sim 10^1$  planetary cores, which contain together about  $60 M_E$  of silicate and ice. During that process, bodies in the disk (especially planetesimals) departed more and more from their in-plane (uninclined), nearly circular orbits in which planetesimals formed near the midplane of the disk.

The cores of proto-Jupiter and proto-Saturn grew to the critical mass of order  $10 M_E$ . Following a nucleated instability of primordial atmospheres, they quickly accreted their massive gaseous envelopes, probably very close in time to the dissipation of the massive gaseous nebula (Lissauer 1993). Rapid core formation (a few million years) requires planetesimal accretion to have proceeded in a runaway regime from a small initial mass up to the critical-mass planetary core. Importantly, the runaway accretion, which ends at a core mass  $\sim \Sigma_p^{3/2}$ , requires a sufficient surface density of the planetesimals,  $\Sigma_p(r)$ , at least several times larger than in the minimum solar nebula. Terrestrial planets are thought to have formed over a time span of  $\sim 100$  Myr (Wetherill 1990).

### 2.5 *Other Possible Outcomes of Accumulation*

The recent discoveries have made it abundantly clear that the range of planetary masses, orbital radii, and orbital eccentricities in other planetary systems is much larger than in our system (and its standard formation theory). While this focuses us on high-mass planets, there may at the same time be many systems that for a very long time look like forming planetary systems, because

they contain millions of planetesimals, but never produce planets. All that is required for this is  $\Sigma(r)$  several times lower than in the minimum solar nebula (e.g. because the nebula is less massive or more extended). Notice that low  $\Sigma$  was the main reason terrestrial protoplanets were never given a chance to become giants. The growth of extrasolar bodies may sometimes be severely slowed down at typical masses much less than that of the Moon, not to mention the Earth or the Jupiter's core. The final stages of planet accumulation in such systems would be prolonged ( $>100$  Myr) and would take place in a largely gas-free environment resembling  $\beta$  Pic.

It is also possible to envisage a successful, rapid formation of planets, followed by their inward migration and ultimate demise inside the star. Orbital migration of an Earth-like planet may occur within the disk (Ward 1986), or a giant planet may migrate within a disk gap cleared by its gravitation (Lin & Papaloizou 1993). Both the gap opening and the migration occur through resonant excitation of spiral density waves in the disk at Lindblad resonances. Small orbital radii of the newly discovered planets (from 0.01 to 0.5 times that of Jupiter) strongly suggest the occurrence of planet-disk coupling in the past. Orbits of super-Jovian planets may become rather eccentric (Artymowicz 1992, Mazeh et al 1997), as may be evidenced by companions to 70 Virginis and HD114762, whose eccentricity is  $\approx 0.4$ . Accumulation of such "super-planets" may occur despite the opening of a disk gap (Artymowicz & Lubow 1996). Therefore, the new theories and observations of other systems permit too wide a range of planetary parameters to yield very specific predictions for  $\beta$  Pic planets. To narrow down the range of possibilities, indirect observational approaches (looking for dust shepherded by planets) should be pursued (see section 3.9).

## 2.6 *Remnant Planetesimal Disks and Clouds*

The fate of up to  $10^{14}$  planetesimals after the disappearance of the gaseous nebula depends strongly on the success or failure of planet formation. In the solar system, planetary perturbations destabilized and removed the planetesimals within a radius of  $\sim 40$  AU (with the exception of the asteroid belt). The clearing period, coinciding with the epoch of giant impacts or heavy bombardment recorded on the terrestrial planets (orders of magnitude higher than the present cratering rate), ended some 800 Myr after the origin of the system (Soderblom et al 1974).

If giant planets did not exist, then the Earth (but not we!) would still be witnessing heavy bombardment by planetesimals and protoplanets, and the distant, spherical, Oort cloud of comets (source of the so-called new comets containing  $10^{12}$ – $10^{13}$  virtually unaltered planetesimals with radii  $> 1$  km, within  $\sim 10^5$  AU from the Sun; cf Lissauer 1993) would not exist. The Oort cloud's

mass is from 10 to a few times  $10^2 M_E$ , and some 20% of the planetesimals from around Neptune were swept out into it. The Oort cloud of today is not directly detectable in the visible or infrared in either our or the  $\beta$  Pic system. During the formation period, however, it was more compact and disk-shaped (Duncan & Quinn 1993). The accompanying dust component could, in principle, be observable in  $\beta$  Pic.

Equally relevant to  $\beta$  Pic is the existence of the Kuiper belt, a relatively undisturbed disk of primordial comets with a sharp inner and fuzzy outer edges (cf Duncan & Quinn 1993, Weissman 1995). Two populations of bodies have been discovered at distances comparable to that of Neptune. Jewitt & Luu (1995) found that  $3.5 \times 10^4$  of large,  $>100$ -km bodies, exist in the Kuiper belt (total mass  $\sim 0.05 M_E$ ), an estimate based on 17 trans-Neptunian bodies in prograde, disk-like orbits. Smaller objects are more numerous:  $>2 \times 10^8$  of them are required in  $<12^\circ$  inclination orbits just outside Neptune, to explain the recent Hubble Space Telescope detection of dozens of Halley-comet sized objects by Cochran et al (1995). Their total mass in the inner Kuiper belt is  $\sim 0.02 M_E$ . Planet formation evidently has failed there because of too little solid material. Is this the story of  $\beta$  Pic disk too? Is it a Kuiper belt that will never form planets? Not necessarily, as we will see shortly.

### 3. OBSERVATIONS AND MODELS OF BETA PICTORIS

The  $\beta$  Pic system consists of three principal, directly observable, components: (a) the star itself, (b) the dust (solid grains with radii  $s \lesssim 100 \mu\text{m}$ ) and sand (up to  $s \sim 5 \text{ mm}$ ) in a disk surrounding the star, and (c) the gas and plasma, probably derived entirely from solids and also gathered in a disk. We discuss the components and the evidence they carry about large unseen bodies orbiting the star, in that general order.

#### 3.1 *The Star*

The central star of the  $\beta$  Pic system has the spectrum of a fairly typical, rapidly rotating main sequence dwarf star of type A5V with effective temperature  $8200 \pm 100 \text{ K}$ . The star's luminosity was found to be significantly less (by 0.3 to 0.8 mag) than that of an average A5V star, a fact that Smith & Terrile (1984) interpreted as a result of gray extinction of starlight by the dust grains in the disk (see, however, Diner & Appleby 1986). Paresce (1991) reconsidered available photometry in terms of an underabundance of metals in the stellar atmosphere (a quarter of the solar metallicity). He also established that  $\beta$  Pic is very near the zero-age main sequence and has existed for  $t_{\text{age}} \lesssim 200 \text{ Myr}$ . Both conclusions were challenged by Lanz et al (1995) who, based on spectral modeling and the assumed grey extinction, placed  $\beta$  Pic on the temperature-magnitude diagram

in a place where  $\beta$  Pic could be a pre-main sequence star, rather than a main-sequence dwarf. This result is controversial: Neither now nor in the recent past has  $\beta$  Pic been in or near any star-forming cloud, it lacks many attributes of pre-main sequence objects, and the assumed dust extinction cannot be reconciled with IRAS data. The best explanation for the difficulties may simply be that the underluminosity is largely an artifact caused by inaccurate knowledge of the distance to the star<sup>2</sup> ( $d = 16.5^{+3.9}_{-2.7}$  pc, cf Kondo & Bruhweiler 1985; the upper limit on  $d$  yields the average luminosity of A5V stars). Holweger & Rentzsch-Holm (1995) observed and modeled  $\beta$  Pic to arrive at the conclusion that it is exactly on the zero-age main sequence and has solar Ca abundance. The bulk of the evidence supports the notion that  $\beta$  Pic is a young main-sequence star with  $t_{\text{age}} \sim 20\text{--}200$  Myr. For comparison, its main-sequence life expectancy is  $\sim 1000$  Myr.

### 3.2 Images of the Scattered Light

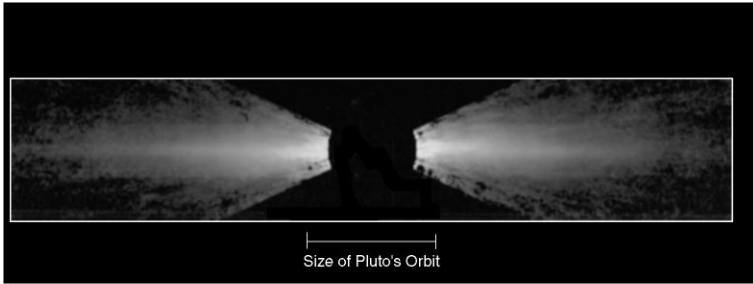
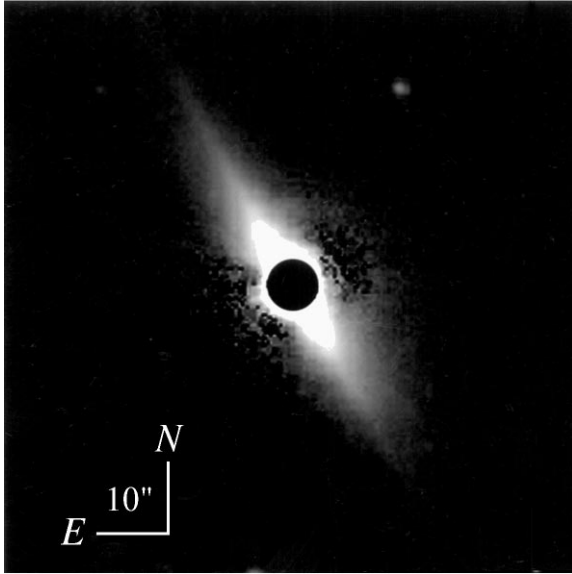
Coronagraphs are used to mask the intense direct starlight. Images of  $\beta$  Pic provided strong direct evidence for the thin light-scattering disk seen nearly edge-on (Smith & Terrile 1984). Two thin disk extensions or wings (NE and SW from the star) reach out to  $> 1000$  AU from  $\beta$  Pic before fading below detectability (Smith & Terrile 1987). A wealth of coronagraphic and other imaging data has since been obtained on  $\beta$  Pic, as recently reviewed by Backman & Paresce (1993) and Artymowicz (1994a). Broad-band spectrophotometry and polarimetry have been obtained, as discussed below. Adaptive optics (Golimowski et al 1993) and anti-blooming CCDs (Lecavelier et al 1993) have also been applied with success.

Figure 1 presents two recent results from ground-based and satellite observations. The top panel shows the R-band (red visible light) image based on observations of Kalas & Jewitt (1995). The inner part of the image (60 AU in this figure) is inaccessible to scattered light imaging because of the intense glare of the star as observed from the ground. The bottom panel presents the Hubble Space Telescope (HST) observations in visible light (filter centered on  $0.55 \mu\text{m}$ ) by C Burrows, J Krist, and the WFPC2 IDT team (cf Burrows et al 1995), reaching down to  $1.5''$  (24 AU) from the star. The main results of the analyses of scattered light images, on which there is some consensus among observers, can be summarized as follows.

The radial profile of the midplane surface brightness of two disk wings is a power-law of the form  $x^\nu$ , where  $x$  is the projected distance from the star, and exponent  $\nu$  appears to change fairly abruptly between the inner ( $x \gtrsim 100$  AU) and outer regions ( $x \gtrsim 1000$  AU). A symmetric change from  $\nu \approx -3$  (inside) to the

<sup>2</sup>The distance of 16.5 pc will be used in this paper, but it must be kept in mind that distances within the  $\beta$  Pic system obtained from telescopic observations are uncertain by up to 20% when expressed in AU.





*Figure 1* *Top:* Two spindle-like extensions sticking out of the image of  $\beta$  Pic present an edge-on view of its dust disk in this R-band image of Kalas & Jewitt (1995). The 10-arcsecond marker gives the scale of  $\approx 170$  AU linear distance, and the black mask has a radius of  $3.7''$ , or 60 AU, that would cover all the planets and currently observed Kuiper belt objects in our system, if placed at the distance of  $\beta$  Pic. (Courtesy of P Kalas.) *Bottom:* The inner region of the disk imaged with the WFPC2 camera on of the Hubble Space Telescope by Burrows et al (1995). NE extension is to the left, SW is to the right. The scale of  $4.8''$  or 80 AU is marked at the bottom. (Courtesy C Burrows and NASA.)

$v \approx -4$  (outside) that was suggested as a possibility by Artymowicz et al (1990), was found by Golimowski et al (1993) to be real and somewhat larger, as well as asymmetric with respect to the center (cf also Kalas & Jewitt 1995). The NE wing of the disk seems to extend further from the star but both wings are almost equally bright at  $x \lesssim 100$  AU. The maximum NE/SW asymmetry at any radius is  $\lesssim 20\%$  of the surface brightness. (Asymmetry should be recognizable by looking at the top panel of Figure 1 and then turning it upside down for comparison.)

Modeling of the observed scattered light distribution has shown that an important quantity, the vertical optical thickness  $\tau(r)$  (percentage of the disk equatorial plane covered by projected area of particles), falls with distance as  $\tau(r) \sim r^{-1.7}$  (or  $\tau(r) \sim r^{-1.9}$  in some models) in the interval  $100 \lesssim r \lesssim 400$  AU (Artymowicz et al 1989, Kalas & Jewitt 1995). The intrinsic vertical density profile of particles in the disk is best modeled by an exponential profile (Kalas & Jewitt 1995, Burrows et al 1995). At  $x \gtrsim 120$  AU from the star, the effective thickness of the disk image grows almost linearly with  $x$ . This requires the disk to have a constant half-opening angle ( $\sim 7^\circ$ , Artymowicz et al 1989), or a slightly flaring profile (thickness  $\sim r^{1.3}$ ). The disk is inclined to the line of sight by  $\sim 3^\circ$  (Kalas & Jewitt 1995). We are thus looking at the star through an optically thin disk (model extinction along any line of sight less than 10%). The image thickness is 25% larger on the SW side of the disk than on the NE side. The distribution of dust thickness may be growing faster on the SW side of the disk, but there may be little asymmetry in the disk when viewed pole-on (Kalas & Jewitt 1995) because it is in the SW part that the midplane profile falls more steeply with  $x$ . Thus, importantly,  $\tau(r)$  determined from scattered light is not subject to substantial asymmetries.

At  $x \lesssim 100$  AU the image thickness becomes NE/SW-symmetric, independent of  $x$ , equal to 30 AU in ground-based images (e.g. Lecavelier et al 1993), and of order 7–10 AU in the HST images. It is not clear whether the scattering efficiency falls rapidly within  $r \lesssim 100$  AU (such that we see the forward scattering from the inner edge of the disk) or, alternatively, the intrinsic thickness of the inner disk becomes constant inside this distance.

Two further asymmetries (Kalas & Jewitt 1995) plague the disk. One of them, called wing-tilt, is understood as an effect of the predominant forward (or much less likely, backward) light scattering by particles in an inclined disk. It causes angular misalignment of wings by  $1.3^\circ$  and allows an estimation of the disk inclination ( $3^\circ$ ). (This asymmetry should be detectable, with the help of a transparent ruler, in the top panel of Figure 1). The other—called butterfly asymmetry by Kalas & Jewitt—is due to a larger amount of dust on the SE side of the NE wing (as compared with its NW side), and on the NE side of the SW wing. Its origin is as little understood as the changes at  $\sim 100$  AU discussed above. A somewhat similar warp-like asymmetry was newly found in

the innermost regions (Burrows et al 1995). As an explanation, it was proposed that the inner disk part has a  $3^\circ$  orbital inclination with respect to the outside disk (seen edge-on to within  $1^\circ$ ). (The warp is present, but difficult to see, in the central part of the bottom panel of Figure 1.) We discuss the interpretation of this feature in the framework of the planetary hypothesis in section 3.9.

The disk light from blue to near-IR (between the B and I bands) matches the color of the star, i.e. the disk is intrinsically gray (Paresce & Burrows 1987, most of Lecavelier et al 1993 spectrophotometry). This excludes the dominance of small (sub- $\mu\text{m}$ ) grains in the disk area and constrains particle composition (see section 3.7).

### 3.3 Infrared Excess from Dust and Sand

Figure 2 shows the observed IR excess fluxes of  $\beta$  Pic and Vega. IRAS data are located between  $12 \mu\text{m}$  and  $100 \mu\text{m}$ . The circumstellar dust of  $\beta$  Pic dominates the stellar photospheric flux starting from the  $12 \mu\text{m}$  IRAS bandpass and peaks in the  $60 \mu\text{m}$  band (cf Gillett 1986). At far-IR and mm wavelengths, the

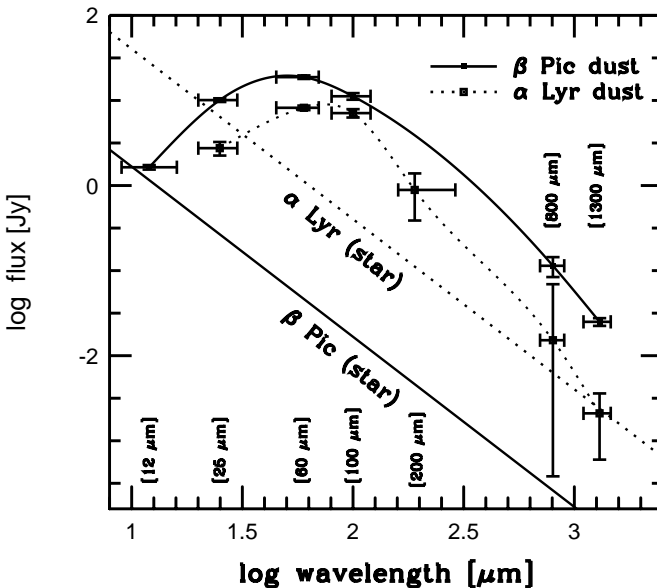


Figure 2 Observed thermal radiation flux (emitted infrared excess) from circumstellar dust in  $\beta$  Pic and  $\alpha$  Lyr (Vega). Stellar photospheric fluxes are shown for comparison. Lines joining the points are a visual aid and do not represent models. (Data from Harper et al 1984, Gillett 1986, Chini et al 1990, Chini et al 1991, and Zuckerman & Becklin 1993.)

dust radiates  $10^2$  more energy per unit frequency than the star. In contrast to  $\beta$  Pic, Vega, a historical prototype of its class, has in fact only a ten-fold far-IR excess, due to a much smaller amount of circumstellar dust. Both excesses peak at wavelengths corresponding to blackbody radiation with temperature  $T \approx 100$  K. However,  $\beta$  Pic's excess is broader than a single Planck curve and requires emission from black bodies (or more realistic materials) with a wide range of temperatures, generally from  $T < 50$  K to  $T \sim 200$  K (Gillett 1986). This range, caused by the radial spread of particles in the disk, is the same as observed in other Vega-type objects, which means that they typically have a large deficit of hot grains ( $T \gtrsim 200$  K) located close to the stars. Both in  $\beta$  Pic and the other systems, grains at temperatures above the efficient sublimation limit of water ice (usually assumed at 150 K; 120 K at  $\sim \mu\text{m}$  size) are rare. The disks have central gaps, holes, or clearing regions which, however, are not necessarily completely empty, as will be seen below. Variable aperture and small detector-array observations, as well as the original IRAS scans, have yielded some information on the spatial extent of the system at wavelengths  $\lambda = 10 \mu\text{m}$ ,  $20 \mu\text{m}$ , and  $60 \mu\text{m}$  wavelengths (Gillett 1986, Telesco et al 1988, Backman et al 1992), and have helped to restrict possible grain sizes in the following way.

Dust is heated by the absorbed stellar UV and visible radiation and cooled via thermal IR radiation (and the usually negligible evaporative losses). The relation  $T(r)$  [or  $r(T)$ ] determines the angular scale of the  $\beta$  Pic disk image in any bandpass. It depends sensitively on grain emissivity  $\epsilon(\lambda)$  dependent on grain parameters. Three simple models for  $\epsilon(\lambda)$  have been used in modeling (Diner & Appleby 1986, Artymowicz et al 1989, Backman et al 1992): (a) constant  $\epsilon$  corresponding to blackbody grains, or large grey grains with radii  $s \gtrsim 10^2 \mu\text{m}$ ; (b) mid-size grain emissivity, decreasing in IR as  $\epsilon = \lambda_0/\lambda$  (where  $\lambda_0 \sim 1 \mu\text{m}$  is correlated with  $s$ ) and constant in the visible. Mid-size grains have difficulty with cooling via thermal emission and are thus hotter than large grains at any radius  $r$ ; (c) emissivity decreasing as  $\epsilon \sim \lambda^{-1}$  in both the visible and IR, representing the properties of small grains, e.g. submicron-sized interstellar grains.

The IRAS and ground-based 10–20- $\mu\text{m}$  observations require the presence of midsize grains (Backman et al 1992) and are inconsistent with either only large grains or only small grains. This does not preclude the presence of large (or small) grains, only their dominance as contributors to the integrated grain area and radiation! On the contrary, evidence has accumulated for a very wide size spectrum of particles. Grains in the range  $s = 100 \mu\text{m}$  to 1 mm have been inferred from  $\lambda = 0.8$  mm observations (Zuckerman & Becklin 1993), and in the range from 6  $\mu\text{m}$  to 4 mm from  $\lambda = 1.3$  mm observations (Chini et al 1991). From the distribution of grain sizes, each observing technique will tend to pick up and emphasize the presence of a “typical” grain size, usually close to the wavelength  $\lambda$  used (much smaller grains do not couple well to

radiation with that wavelength). In the case of submillimeter and millimeter radio observations, we study the sand particles that should contain the bulk of the directly observed mass.

In the standard  $dN \sim b^{-3.5} db$  size distribution of particles in collisionally evolved systems, most mass is in the largest particles, and most area in the smallest. Indeed, the total of at least  $0.13 M_E$  of dust and sand follows from the  $\lambda = 0.8$  mm observations, and at least  $0.5 M_E$  ( $3 \times 10^{27}$  g) is found in the  $\lambda = 1.3$  mm work. Because the ratio of wavelengths in millimeters and optical observations and, hence, the ratio of grain sizes studied is  $\sim 10^3$ , the ratio of masses derived should be  $10^{3/2} \approx 30$  if the  $s^{-3.5}$  distribution applies. For comparison, the optical/far-IR models discussed in section 3.6 yield a minimum dust mass of about  $1/300 M_E$ , or roughly 70 times smaller than the millimeter work indicates. This is consistent with the idea that  $\beta$  Pic dust is but a part of a steady-state collisional cascade of planetesimals  $\rightarrow$  rocks  $\rightarrow$  pebbles  $\rightarrow$  sand  $\rightarrow$  dust, with the standard power-law size spectrum extending over at least three decades in size from dust to sand. Naive extrapolation of this power-law by another 5.5 decades from  $\sim 0.3$ -cm sand to 1-km planetesimals yields a total mass of  $\sim 140 M_E$ , consistent with the total mass of planetesimals derived in section 2.3. This indicates that either the standard collisional hierarchy ends at the planetesimal size, and there are no planets, or that the power law becomes steeper and extends to many-kilometer bodies.

### 3.4 Direct Thermal Imaging

Based on the IR data, the size of the inner disk clearing could be estimated at 20–40 AU in very simple power-law models of radial density distribution (cf Backman & Paresce 1993). Better knowledge of the conditions in the gap region came with IR observations at  $\lambda \geq 12 \mu\text{m}$ , which do not require coronagraphic masking. Utilizing sophisticated image reconstruction techniques, Lagage & Pantin (1994) were able to achieve resolution of order 5 AU. Figure 3 (*top*) presents the 10.5–13.3  $\mu\text{m}$  bandpass image of  $\beta$  Pic system (Pantin 1996). The dust forms a thin structure, probably a non-uniform disk around the star (located in the center of the bright circular spot). Comparing this image with scattered light images (e.g. Figure 1) one can notice a large qualitative difference: The thermal flux increases toward the star much more slowly than the scattered flux. This difference can be attributed to the strong forward scattering of micron-sized grains, as opposed to the isotropic thermal emission. The latter is thus more readily convertible to the radial dust distribution but, on the other hand, still does depend on the grain emissivity  $\epsilon(\lambda)$ , determining the  $T(r)$  relation. The lack of a steep rise of IR emission flux near the star, despite its large sensitivity to changing grain temperature, means that the dust is much depleted in the immediate surroundings of the star.

Figure 3 (*bottom*) shows the projected dust distribution inferred from the top panel under certain model assumptions (grain temperature follows the same function of the projected distance as the radial dependence expected of astronomical silicates with properties given by Draine & Lee 1984). The inner void of matter and the asymmetries reported earlier by Lagage & Pantin (1994) are evident in this figure. The SW/NE ratio of thermal emission from the dust peaks at the value of  $2.8 \pm 1.4$  at a projected distance of 60 AU from the star but becomes close to unity between 80 and 100 AU. The scattered light, as noted, is very symmetric by comparison, maybe because it originates at a larger radius  $r$  in the main disk, and is scattered through a small angle to be seen at  $x \ll r$ . The  $12 \mu\text{m}$  flux in Figure 3 is observed as far from the star as  $r = 100$  AU. This entails a  $T(r)$  relation keeping the grains at a relatively high temperature at such  $r$  and indicates dark materials, small grains sizes, and/or a fluffy structure such as may exist in cometary grains (Greenberg & Hage 1990).

The modeled distribution of optical thickness  $\tau(r)$  in the innermost region is rather uneven, but on both sides the values deduced at  $r = 20$  AU are  $\tau(r) \lesssim 10^{-3}$ , a factor of five smaller than those in the relatively flat-profile region  $r \gtrsim 50$  AU (Lagage & Pantin 1994; E Pantin, PO Lagage & P Artymowicz, in preparation). The gap half-clearing radius of 20–30 AU is roughly consistent with the coronagraphic constraints.

### 3.5 *Silicates in the Gap Region*

Although we have treated IR radiation as thermal continuum, there is one notable exception: warm silicates ( $T \sim 300$  K) producing a well-known  $10\text{-}\mu\text{m}$  emission feature (the Si-O stretch mode) have been found spectroscopically by Tesesco & Knacke (1991), and studied further by Aitken et al (1993), and Knacke et al (1993). Judging by the approximate temperature and location, the same particles may cause this emission feature and the thermal flux in Figure 3. The same can be concluded from the fact that only  $\sim 3 \times 10^{21}$  g ( $\sim 10^{-6} M_E$ ) of silicates are required to produce the observed intensity of the line, i.e. only  $10^{-4}$  of the total dust mass (or  $10^{-6}$  of the sand mass) in the disk.

As shown in Figure 4, the overlapping broad  $9.6\text{-}\mu\text{m}$  and weaker  $11.2\text{-}\mu\text{m}$  emission features agree with the solar system cometary analogs, especially well with Halley's comet dust feature peaking at  $9.8 \mu\text{m}$  and  $11.3 \mu\text{m}$ . In fact, none of the astronomical objects such as interstellar medium grains, interplanetary dust particles (IDPs, cosmic particles collected in the stratosphere and elsewhere on Earth), or circumstellar disks provides a better fit. This is an important clue. Halley's feature is due to silicates: A mixture of polycrystalline silicates seems to fit the data [56% of olivine, 36% of pyroxene, and 8% lattice-layer silicates (cf Bregman et al 1987, Campins & Ryan 1989) or, alternatively, 95% amorphous olivine with cosmic abundances and 5% crystalline olivine (Blanco et al 1991);

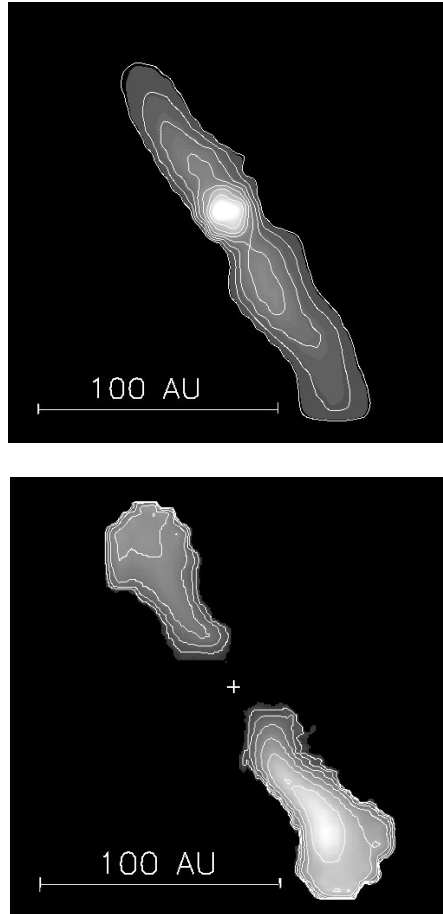


*Figure 3* *Top panel:* Innermost part of the  $\beta$  Pic system observed in the infrared 12- $\mu$ m band with  $\sim 5$ -AU resolution. The neighboring isophotes show surface brightness differing by a factor of two. The thin disk structure is aligned with the optical disk (Figure 1). However, it is much more asymmetrically distributed with respect to the star (the bright spot). *Bottom panel:* Dust density map deduced from the observed flux, adopting a power-law size distribution of silicate grains and the projected distance from the star (denoted by a cross) as a basis for the temperature calculation. (Courtesy of E Pantin.)

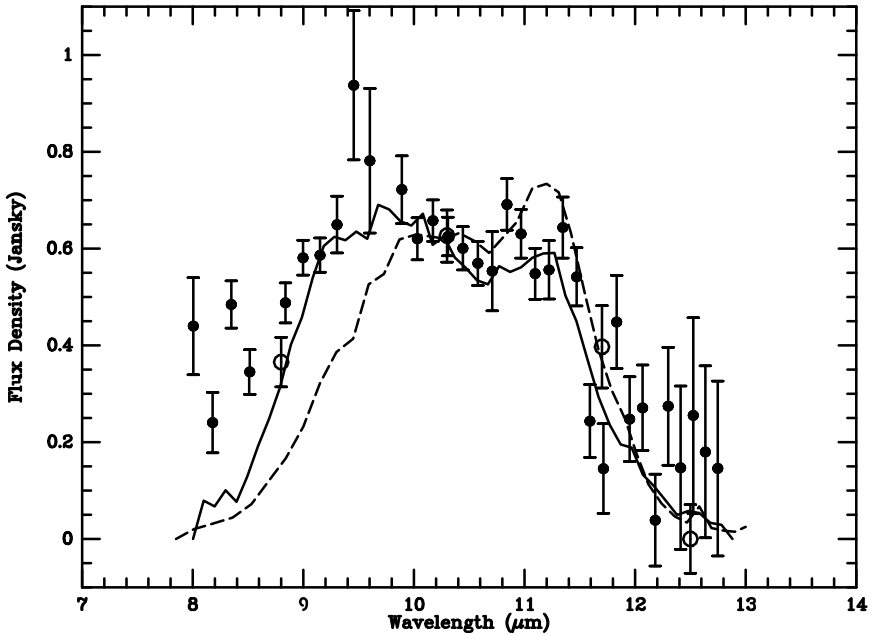


Figure 4 The broad  $10\ \mu\text{m}$  emission feature of warm  $\beta$  Pic silicates (points), compared with spectra of comet Halley (solid line) and comet Levy 1990 XX (dashed line), after subtraction of the cometary continuum. The spectra were normalized at the  $10.3\text{-}\mu\text{m}$  point. (Courtesy R Knacke and S Fajardo-Acosta.)

however Sandford (1991) argues that only crystalline olivine and pyroxene are dominant]. Amorphous or polycrystalline silicates may cause the stronger line component at  $9\text{--}10\ \mu\text{m}$ , whereas the crystalline olivine may be responsible for the weaker  $11.2\ \mu\text{m}$  feature in  $\beta$  Pic. The upper limit on radii of compact silicates is  $s \approx 1\text{--}2\ \mu\text{m}$  (e.g. Knacke et al 1993, Aitken et al 1993, Artymowicz 1994a; if significantly porous, particles could be a few times larger than this).

At this point, unique identification of all minerals involved is still impossible. However, the leading candidate materials (olivines, pyroxenes) are the building blocks of the solid bodies in the present solar system and are anticipated in  $\beta$  Pic based on cosmogony and astrochemistry (section 2.2).

### 3.6 Distribution of Grains from Combined Visible and Infrared Modeling

Simultaneous modeling of the scattered and the reemitted IR radiation is necessary for reconstructing the spatial density and composition of particles. Simple



power-law emissivities of midsize grains (section 3.3), and assumed axisymmetry of  $\tau(r)$  have been employed most notably by Artymowicz et al (1989), and Backman et al (1992) to determine the radial distribution of grains in the disk, including the central gap. The methods, and some results, were different among the studies.

Artymowicz et al (1989) attempted a one-component model of the disk, i.e. assumed uniform grain properties throughout the disk. They inverted the integral equation for the observed IR flux to obtain the distribution of grain area as a function of temperature  $A(T)$ , and then the radial distribution of solid matter within the disk. They used a non-parametric Maximum Entropy Method (MEM), which does not predefine any functional form for the dust distribution (in temperature or radius) but finds it requiring that the resultant distribution is as featureless as possible (maximum entropy) while remaining consistent with the data to within the observational error. For a range of grain emissivity models, MEM inversion places the half-clearing point of the disk at a temperature  $T = 160$  K and indicates that the density maximum coincides with  $T = 95\text{--}115$  K, allowing, in principle, the main disk (but not the gap region) to contain stable water ice. The total cross-sectional area of all the grains is very impressive in these and other published models:  $\sim 10^3$  AU<sup>2</sup>, i.e. a circle of 20 AU radius, or the area of Uranus' orbit. For an effective dust particle radius  $\sim 4$   $\mu\text{m}$  and density of  $1$  g cm<sup>-3</sup>, this yields a lower limit on the dust mass equal to  $3 \times 10^{25}$  g or  $4 \times 10^{-3} M_E$ .

Backman et al (1992) introduced first a two-particle model of  $\beta$  Pic disk, where inside the  $r = 80$  AU dividing line, the grains were allowed to have different properties (resembling the refractory dust) than outside (where brighter particles can exist). They used a piece-wise power-law spatial distribution of grains and determined the free parameters such as inner radius, normalization, and power indexes, to be determined from observations by a least-squares fit. Artymowicz (1994a) argued that MEM is preferable to parametric modeling, pointing out some suspicious features of the few-parameter models<sup>3</sup>.

For the estimates of collisional and other timescales (section 4.4) we need to quantify the total  $\tau(r)$  (due to all grain types and sizes). We introduce a simple mathematical description of the  $\tau(r)$  (from all grain types and sizes) patterned after the preferred MEM solutions (e.g. the midsize-grain model 7 of Artymowicz et al 1989) and consistent to within  $\sim 30\%$  with other available modeling, showing that dust area decreases as  $r^p$  toward the star within  $r \lesssim 40$  AU ( $p = 1$  suggested by visible HST observations,  $p = 2$  better representing

<sup>3</sup>The irony here is that simple parametric models suggest a bimodal grain distribution (which may be true), but without providing sufficient proof. If, instead of assuming inflexible power-laws, we let MEM choose  $\tau(r)$ , it is able to converge to a smooth radial solution with just one grain type!

the 12  $\mu\text{m}$  map inversions). The optical thickness is approximately equal to the following:

$$\tau(r) = 2\tau_m / [(r/r_m)^{-p} + (r/r_m)^{1.7}], \quad (1)$$

where  $r_m = 50$  AU is a characteristic radius within which density drops and  $\tau_m = \tau(r_m)$  is the characteristic optical thickness there. We shall mostly consider  $p = 2$ , for which the maximum density equal  $1.003\tau_m$  is reached at  $r = 1.045r_m$ . In order for our particle distribution to intercept the correct percentage of the starlight (reproducing the total IR excess to the stellar luminosity ratio of  $L_{\text{dust}}/L_* = 2.4 \times 10^{-3}$  for  $\beta$  Pic), we require  $\tau_m = 8.5 \times 10^{-3}$  (assuming that 33% of incoming stellar flux is absorbed by grains).

COMPARISON WITH ZODIACAL DUST DISTRIBUTION It is fascinating to compare the distribution of dust in  $\beta$  Pic disk and its closest analog in the Solar System – zodiacal light (ZL). Interestingly, like  $\beta$  Pic disk, ZL has a nearly exponential (sharply centrally peaked) vertical profile with scattering area proportional in one model to  $\exp[-4.2(z/r)^{1.2}]$  (Good et al 1986). It is also inclined to the ecliptic and the invariant plane by a few degrees and is slightly warped [due to inclined dust sources (asteroids producing so-called IRAS dust bands)], probably to adjust to local orbital planes of the planets. However, ZL forms a thicker structure since the vertical profile has a scale height as large as  $z = 0.3r$ , two to three times larger than in  $\beta$  Pic. Zodiacal dust, unlike most of the  $\beta$  Pic disk, has a fairly uniform radial distribution (at least in the inner solar system) expressed as  $\tau \sim r^{-0.3}$  to  $\tau \sim r^{-0.1}$ . Finally, the normalization of  $\tau$  throughout the planetary region of our system is close to  $\tau = 10^{-7}$ , or  $\lesssim 10^{-4}$  of typical  $\beta$  Pic's value (cf Equation 1). The differences likely mirror the different spatial density distribution of parent bodies in the respective systems, but not the basic nature of the phenomenon.

### 3.7 *The Nature of Grains in the Disk*

We concentrate in this section on the densely populated area outside the inner clearing (at  $r \gtrsim r_m/2 \sim 30$  AU).

ONE OR MORE GRAIN POPULATIONS? As already mentioned, some parametric models featured two grain populations on opposite sides of an assumed boundary. A discontinuous radial profile of the absorbing area in those models and a continuous scattering grain area (section 3.2) require at least one darker (silicates?) and one brighter (ice?) material for the grains. On the other hand, the nonparametric models do not require (or contradict) any sharp divisions or fractionation. Although the situation is still not completely clear, preliminary modeling based on IR mapping (E Pantin 1996; E Pantin, PO Lagage &

P Artymowicz, in preparation) does favor two separate or intermixed populations of particles, each having a different  $T(r)$  dependence. As discussed in sections 3.2 and 3.4, the IR imaging shows much larger asymmetries inside  $x = 100$  AU than does the coronagraphic imaging, suggesting that different particles are responsible for most absorption and for most scattering. Secondly, the high temperatures of dust inside the gap, required by the spatial scale of the  $12 \mu\text{m}$  radiation, are most easily, though perhaps non-uniquely, modeled with micron-sized, very porous, particles proposed to constitute cometary material in the Solar System (Greenberg & Hage 1990), and in the  $\beta$  Pic system (Greenberg & Li 1996). Comet-derived, porous chondritic IDPs (super-rich in carbon) have been studied in laboratories (cf Rietmeijer 1992). Their optical properties, especially the predicted very dark appearance (albedo<sup>4</sup>  $A < 0.1$ ) are inappropriate for the outer disk modeling (see below), supporting the necessity of a dual composition of  $\beta$  Pic dust. The quantity and quality of data available until recently was insufficient to make an attempt at self-consistent modeling with real material properties, multiple-component disk, and flexible dust distribution. Accordingly, most existing models could only derive properties of “average particles.”

**COMPOSITIONAL CONSTRAINTS FROM ALBEDO AND COLOR** The average albedo  $A$  of the outer disk was, for a brief period of time in 1980s, wrongly suspected to be small,  $A \lesssim 0.1$ , like that of many solar system objects: comet Halley’s nucleus; undifferentiated asteroids of class C, B, and G; many carbonaceous chondrites; or the rings of Uranus. This was in part suggested by an empirical relation between  $A$  and polarization for meteorite and asteroidal surfaces, which in general does not hold for dust (McDonnell et al 1991). The conclusion, based on combined visible/IR models, that  $A \approx 0.5\text{--}0.9$  (Artymowicz et al 1989) was confirmed in later work (with some downward reduction to  $A \approx 0.5 \pm 0.2$ , cf Backman et al 1992, Pantin 1996, Burrows 1996).

The high albedo conveys an important message about mineralogy. Unlike in the gap region ( $r \lesssim 30$  AU), grains of intrinsically dark, absorbing materials [iron-rich oxides and silicates, including the “astronomical silicates” of Draine & Lee (1984)], carbonaceous and organic compounds, and pure metals, are inadequate for the particles in the disk, simply because they are too dark and too red in appearance. The disk seen in Figure 1, if composed of such materials, would absorb rather than scatter most of the stellar radiation and reemit too much thermal continuum compared with the data in Figure 2. The dominant materials have large and constant (to within 10%) reflectivity in the visible range. Based on these criteria and reflectance studies of fine-powdered samples, Artymowicz et al (1989) proposed feldspars, olivine (forsterite), or alternatively

<sup>4</sup>We do not consider diffraction as part of scattering, otherwise all the visible albedos (scattering/extinction ratios) would be nominally  $A > 0.5$ .

“astronomical” ices ( $\text{H}_2\text{O}$ ,  $\text{CO}_2$ ,  $\text{NH}_3$ ,  $\text{CH}_4$ ) darkened by a small amount ( $< 1\%$ ) of carbonaceous material. (The icy composition option encounters theoretical difficulties outlined below in section 4.6).

The single most important parameter controlling the albedo and color of the silicates is the  $\text{Fe}:(\text{Fe} + \text{Mg})$  ratio. Iron-rich silicates, due to the presence of  $d-d$  electronic transitions within the  $3d$  orbital of  $\text{Fe}^{2+}$  ions, have a red and dark appearance (depending on the size distribution of particles, they may show characteristic deep broad absorption features near  $1 \mu\text{m}$  from olivine and in addition near  $2 \mu\text{m}$  from pyroxenes). In contrast,  $\text{Mg}^{2+}$  ions lack the necessary  $d$  electrons, and thus magnesium-dominated silicates are practically as transparent and colorless as ices at visible wavelengths (up to the wing of a UV absorption edge). Materials such as anhydrous olivines and pyroxenes with relative mass content  $\text{Fe}:(\text{Fe} + \text{Mg}) \lesssim 0.2$  are excellent gray-colored scatterers suitable for modeling the bulk of  $\beta$  Pic disk grains. An additional parameter determining albedo and radiation pressure is the percentage of carbon: Very small volume fractions are known to considerably darken micronic grains of silicates and ices. As with Fe, the abundance of C must be much smaller ( $\lesssim$  few percent by volume) than in the interstellar or cometary grains.

**LINEAR POLARIZATION** The linear polarization vector of scattered light measured at  $x \gtrsim 140$  AU is oriented perpendicular to the disk wings (as expected of a dust disk). The values of polarization in B, V, R, and I bands are in the range from 13–17% (Gledhill et al 1991, Wolstencroft et al 1995). A possible minor increase of polarization with  $x$  and stronger SW wing polarization are indicated by some data, with little dependence on the color.

We can inquire whether the interplanetary silicates from the Solar System (Bradley et al 1988), such as zodiacal light (ZL) dust, IDPs, and cometary dust, would reproduce the visible polarization data in the outer  $\beta$  Pic disk, if distributed according to Equation 1 (and within an appropriate vertical thickness). A positive answer is provided in Figure 5, where we have compared the visible band-pass data from Wolstencroft et al (1995) with a simple model computed as follows. We have used the empirical volume scattering phase function  $f(\theta)$  and the polarization function  $P(\theta)$  (where  $\theta$  denotes the scattering angle) of (a) the ZL disk at 1 AU from the sun (insets, Lamy & Perrin 1991), and (b) typical cometary coma grains.<sup>5</sup> We have computed the distribution of polarized components of the scattered flux projected on the sky, assuming a small ( $1^\circ$ ) inclination of the disk, and plotted the midplane values of the resultant polarization as solid

<sup>5</sup>Our smooth  $f(\theta)$  and  $P(\theta)$  functions interpolate/extrapolate among data in Ney & Merrill 1976, and Dollfus et al 1988; these data have somewhat restricted  $\theta$ -coverage and thus give less reliable results. However, cometary particles have similar polarization curves as IDPs (Levasseur-Regourd et al 1990) and meteoritic dust samples (Weiss-Wrana 1983) for which more data exist.

lines in Figure 5. The presence of a gap and variations in disk thickness cause the polarization to decrease for  $x \gtrsim 100$  AU and to be higher away from the midplane (maximum values given by the dashed lines). A slow rise of  $P(x)$  at large distances is caused by the assumed outer disk boundary at  $r = 1000$  AU. The observed polarization is consistent with that which would arise from ZL, and similar to that of IDPs or cometary grains. In view of the well-known sensitivity of linear polarization to grain size distribution and surface roughness, it is likely that the dust in the solar and  $\beta$  Pic systems has similar properties. Particle size distributions may be somewhat different in the SW and NE disk sections because  $P(x)$  is not a symmetric function (Wolstencroft et al 1995).

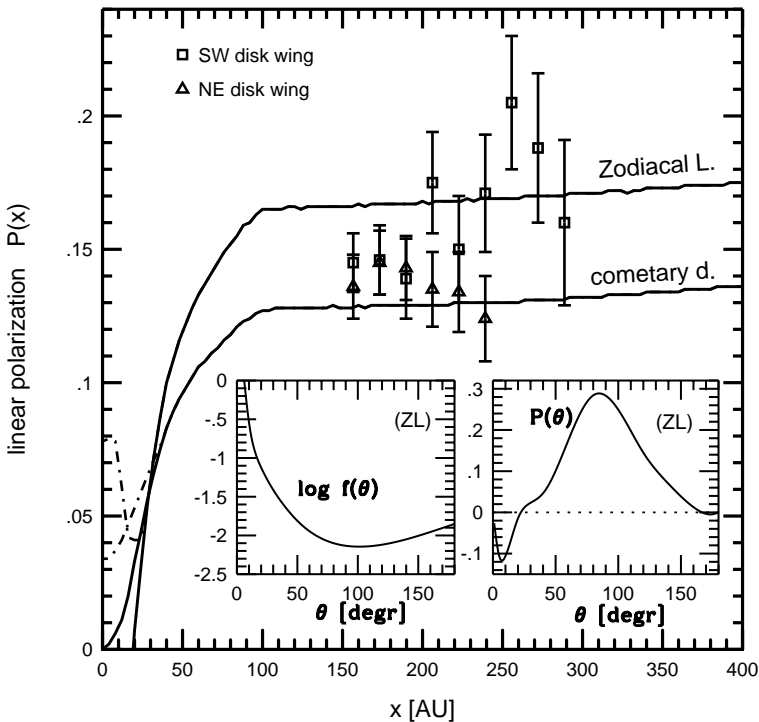


Figure 5 Visible linear polarization (data from Wolstencroft et al 1995), shown separately for the two extensions of the  $\beta$  Pic disk as a function of projected distance from the star (points with error bars). Insets show the empirical phase function and polarization of zodiacal light dust in the vicinity of Earth (Lamy & Perrin 1991), which were used together with the disk density model discussed in the text to derive the solid theoretical curve ("Zodiacal L."). The second theoretical curve ("cometary d.") is based on similar data for an average cometary dust particle.

ON THE NATURE OF GRAINS All the candidate materials for  $\beta$  Pic grains, both inside and outside the main disk (olivines and pyroxenes of various sizes and crystallinities) are very similar to those actually found in the Solar System. Moreover, the empirically proposed composition fits very well with the a priori expectations for abundant  $\beta$  Pic minerals (section 2.2).

While it is generally very difficult to make a direct comparison between the theoretically (un)known dust density in an early Solar System and the directly observed  $\beta$  Pic dust density, a comparison of the composition and mineralogy of dust is simpler. Unlike the dust densities we do not expect the composition and mineralogy to substantially change over time. Both now and in the past, dust grains represent fragments of essentially the same comets and asteroids formed in the protoplanetary disk. The fact that the dust in  $\beta$  Pic appears very similar to some Solar System materials reassures us of the basic similarity of the two systems.

The albedo of  $\beta$  Pic materials (in the main disk) is noticeably higher than in typical IDPs or astronomical silicates. If true, what could be the reason for this difference? There are possible ways in which the semitransparent glassy silicates could have become abundant in  $\beta$  Pic. In the condensation sequence, enstatite and forsterite are among the most abundant higher-temperature equilibrium minerals between approximately 400 and 1400 K. Such minerals could form quickly in a cooling nebula and remain unaltered by low-temperature inclusion of iron, pyrite, water, etc because there was insufficient time (owing to kinetic inhibition), and dark and bright grains remained separate. Alternatively, radiation pressure, whose manifold role in disk dynamics is described in section 4, may have selectively depleted the darker, Fe/C-rich grains by blowing them out into the interstellar medium. It is more difficult to interpret the high albedo if planetary systems form retaining weakly altered or unaltered interstellar grains, such as glassy silicates with embedded metal and sulphide inclusions (GEMS; cf Martin 1995), rather than separate fractions of ferritic, carbon-rich, and siliceous grains.

### 3.8 *The Gas and the Evidence for Planetesimals*

The gaseous component of the disk around  $\beta$  Pic reveals its presence spectroscopically via narrow absorption lines superimposed on the broad photospheric lines originating in the rotating stellar atmosphere. Many recent reviews and results on the gas in  $\beta$  Pic can be found in Ferlet & Vidal-Madjar (1994). Below we provide a brief account of some noteworthy results and implications of three types of absorption features that have been observed: (a) stable ones, at the stellar radial velocity and corresponding to a permanent gaseous disk, (b) slowly varying lines, at small shifts of few tens of kilometers/second, and (c) rapidly variable high-velocity features, reaching shifts in excess of 100 km/s.

**STABLE ABSORPTION LINES**  $\beta$  Pic has long been classified as a “shell star” exhibiting the presence of narrow absorption lines of singly ionized metals superimposed on the very broad photospheric lines originating in the rotating stellar atmosphere. These lines originate mainly in ionized species such as Ca II, Mn II, Fe II, and Zn II, but also in neutral species (e.g. Na I, C I, CO) (Vidal-Madjar & Ferlet 1994, Lagrange 1994, Lagrange et al 1995, Mouillet & Lagrange 1995). The basic result is that the column densities of these elements [from  $(3-4) \times 10^{14} \text{ cm}^{-2}$  for Fe down to  $2 \times 10^{12} \text{ cm}^{-2}$  for Ca and  $\leq 3.2 \times 10^{11} \text{ cm}^{-2}$  for Zn] are all in the cosmic (solar) abundance ratios. This observed gas is not derived from a solar-abundance gas like that of the primordial solar nebula, however. Direct upper limits on hydrogen density allow  $\lesssim 1.6 M_E$  of hydrogen around the star, which, compared with the minimum dust and sand mass of  $0.5 M_E$ , gives an upper limit of the gas:dust ratio of order unity, i.e.  $10^2$  times lower than in the solar nebula. For the fiducial  $\sim 120 M_E$  of solids, the gas:solid ratio is less than 1:100. According to R Liseau & P Artymowicz (in preparation), the CO/H ratio may be cosmic, which, coupled with their limits on total CO mass from mm-wavelength observations, gives overall gas:dust mass ratio of only  $\lesssim 0.003$ , or  $\lesssim 3 \times 10^{-5}$  times that in the solar nebula. Thus, the disk is almost gas-free. The likely source of gas is evaporating solid dust grains and macroscopic bodies.

**EVIDENCE FOR PLANETESIMALS FROM VARIABLE ABSORPTION LINES** Indirect evidence for the conversion of solid bodies (with abundances and masses corresponding to 1-km planetesimals) into hot plasma near the star was found in the time-variable absorption features (for review see Vidal-Madjar 1994, Lagrange 1995). The absorption events may last from hours to many days, the more rapid ones involving as a rule higher velocities and also higher ionization of atoms. The absorption is almost always redshifted by up to  $+300 \text{ km/s}$ , about one half of the free-fall velocity onto the star, but more commonly reaches an infall velocity ten times smaller. Some blueshifted events also occur at up to  $-60 \text{ km/s}$  (e.g. Bruhweiler et al 1991). The situation is very complex and sometimes difficult to interpret (Boggess et al 1991, Lagrange 1994). However, the fact that the observed ions feel a much stronger radiation pressure than gravity from the star (especially Ca II, for which the radiation pressure is  $\beta = 77$  times gravity) indicates clearly that the rapidly infalling plasma is the material “boiled off” of infalling large solid bodies. This scenario for episodic absorption events is called Falling Evaporating Bodies or FEBs (Vidal-Madjar et al 1994, Beust 1994, Beust et al 1994). For almost a decade, FEBs have remained the only viable explanation for most observed facts, for instance that the redshifted line doublets have the same strength (they are both optically thick, but the plasma cloud does not cover the whole stellar disk; the dense cloud is essentially a

large cometary coma). The required evaporated mass per event (if abundances appropriate for planetesimals are adopted) usually corresponds to  $s \sim 1$ -km planetesimals. The mass falls in aperiodically, 2–3 times per week, or up to 200 times per year (however, much less than that during some years). This, together with the large predominance of redshifted over blueshifted features, suggests that the FEBs belong to an orbital family (perhaps fragments of a disintegrated large comet) with the mean orbit oriented in such a way that bodies approach the star when they are seen against it.

Figure 6 presents the results of FEB simulation, which reproduces qualitatively some rapidly variable (on timescale of hours) substructure in the low-velocity events, which were observed to last for weeks. The model predicts that small 100-m cometary family members go in and out of view in a matter of hours, the whole family passing within weeks. Detailed hydrodynamical simulations of the FEB comae (depicted in Figure 6 by clouds of dots) clarified the physical conditions of shocked gas, leading to high temperatures in excess of  $10^4$  K, and the resultant observed appearance of highly ionized species like

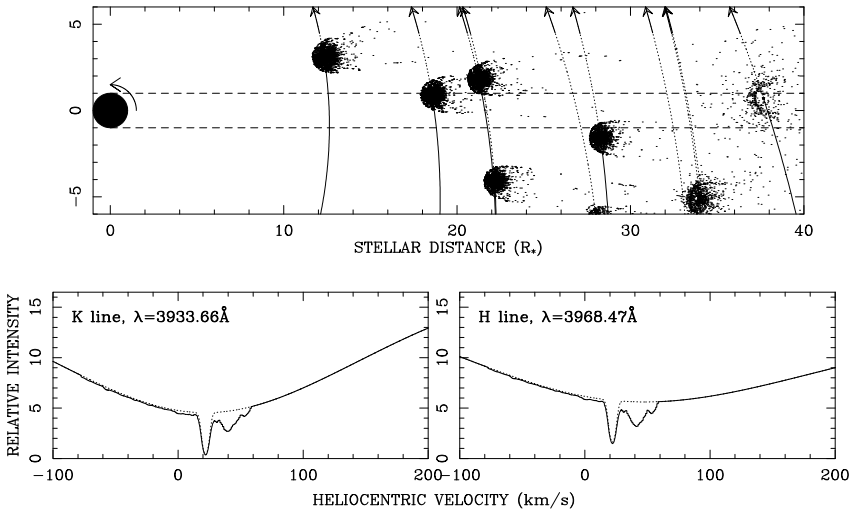


Figure 6 *Top panel:* Simulated view of an orbital family of falling evaporating bodies (FEB: planetesimals, comets) passing in front of the star (black circle at the origin; Earth is to the right). Each comet evaporates creating a coma filled with dense gas containing singly ionized calcium, occulting a fraction of the stellar disk. *Bottom panels:* The cometary comae from the top panel cause single or (as in the top panel) multiple, redshifted, variable absorption features superimposed on both the stable narrow circumstellar and the broad surrounding stellar K and H lines of Ca II (shown by dotted line; both at +22-km/s heliocentric velocity). The simulated redshifted line components explain some observed spectroscopic events in  $\beta$  Pic. (Courtesy of H Beust.)



AI III or CIV (cf Beust 1994). Although it is successful in most respects, it is not clear whether the FEB scenario can account for all the complexity seen in the circumstellar gas surrounding the star. For instance, the origin of the slowly-varying features and the stable component are still not completely understood (Vidal-Madjar & Ferlet 1994, Lagrange 1994). It seems that at least a part of the stably orbiting gas is the high-velocity gas from evaporating bodies decelerated, mixed with, and confined by the disk. But it is an open question exactly how much of the stable gaseous disk is produced by FEBs and how much by the dust.

### 3.9 Planets: Do They Exist?

At present there are no direct or unambiguous indirect indications for the presence of planets around  $\beta$  Pic. However, taken together, the individual arguments discussed in this section make their existence plausible and even likely. For one thing, both the star and the disk are sufficiently mature to have planets (sections 3.1 and 4.5). Further motivation for a planet search in  $\beta$  Pic is provided by normal stars having planets (section 1). The mere existence of planetesimals, however, cannot be used as an indicator that planets necessarily must be forming or have formed (section 2.5).

WHAT CAUSES THE OBSERVED DISK THICKNESS? The half-opening angle of the disk, or in other words the dispersion of orbital inclinations of dust and its parent bodies, was noted to be of order 0.1 rad. This may require the presence of numerous ( $10^2$ – $10^3$ ?) Moon-sized bodies in the disk. They must be small enough not to cause a void of matter around them (we know there are no giant planets outside  $r \sim 100$  AU; their gravity would destroy the smooth power law of disk brightness). At the same time, the large bodies must be able to establish a vertical velocity dispersion of smaller bodies surrounding them on the order of 0.1 times the Keplerian circular speed. The required escape speed from the surfaces of the largest bodies corresponds to (very roughly) Lunar-class perturbers. However, the time dependence of the velocity dispersion may be important, and the necessary theory is not yet fully developed, even for our Solar System (though Nakano 1988 attempted a simple description of the evolution of  $\beta$  Pic-type disks).

WHAT CAUSES FALLING EVAPORATING BODIES TO APPROACH THE STAR? Many researchers consider the existence of at least one planet as necessary for the very existence of FEBs. Namely, the only force able to rearrange the orbital distances and eccentricities of initially nearly circular orbits of planetesimals (similar to orbits of most Kuiper disk objects) is the force of gravity of planets. Nothing short of planets is able to do it efficiently because, for example, comet-sized planetesimals are only able to perturb their orbits to a relative speed (of

order escape velocity) measured in meters per second, rather than the required kilometers per second.

Specific models of how FEBs could originate by perturbation from planets have been proposed by several groups, most notably by Levison et al (1994) and Beust & Morbidelli (1996). The former model invokes secular resonances known in the context of our Solar System (e.g. the  $\nu_6$  resonance is effective at supplying the inner Solar System with collisional debris from the asteroid belt). Secular resonance requires a commensurability of the precessional period of a planetesimal with one of the precessional eigenfrequencies of the planetary system. The result is that planetesimals can approach the star closely on orbits of large eccentricity that are approximately aligned with the periastron of one of the planets (for a secular resonance there must be at least 2 planets). Such a geometry and, in addition, an appropriate viewing angle, are required in  $\beta$  Pic to explain the 9:1 dominance of redshifted to blueshifted absorption events. Beust & Morbidelli (1996) argued, however, that the efficiency of secular resonances is specific to our Solar System, and should not be assumed in  $\beta$  Pic. Instead, they have proposed that 1:3, and particularly 1:4 mean motion resonances of planetesimals with one massive planet on an eccentric orbit ( $e > 0.05$ ) provide a generic and efficient mechanism for the generation of star-grazing orbits. The mechanism does not depend sensitively on either the mass or its orbital distance, and confines the orientation of star-grazing FEB orbits. However, the authors point out a problem of time-scales that is somewhat troubling for their, as well as other, theories. The mechanism changes the orbit slowly enough that repeated passages at larger distances from the star should evaporate the body long before it comes as close to the surface as deduced from observations within the FEB scenario, yet, rapidly enough so that the resonance must be continually supplied with fresh planetesimals. Additional hypotheses are necessary to answer these concerns (Beust & Morbidelli 1996).

PHOTOMETRIC VARIABILITY OF THE STAR Lecavelier et al (1995) analyzed archival photometric observations of  $\beta$  Pic and noticed variations in the brightness of the star with no measurable color dependency. The most interesting of these was an unusual brightening by (only!) 0.04 mag within  $\pm 10$  days from November 10, 1981. We reproduce these puzzling observations in Figure 7. Lecavelier et al (1995) admit that stellar activity of some kind might account for the small variations seen. However, they propose that the variation might well have been produced by a giant planet passing in front of the stellar image. The brightening (due to the Roche lobe of the planet being dust-free) would then be followed by a planetary transit (decrease of brightness) and again, symmetric brightening. The required area of the planet is about four times Jupiter's area, and the distance from the star at least 0.08 AU. This explanation immediately

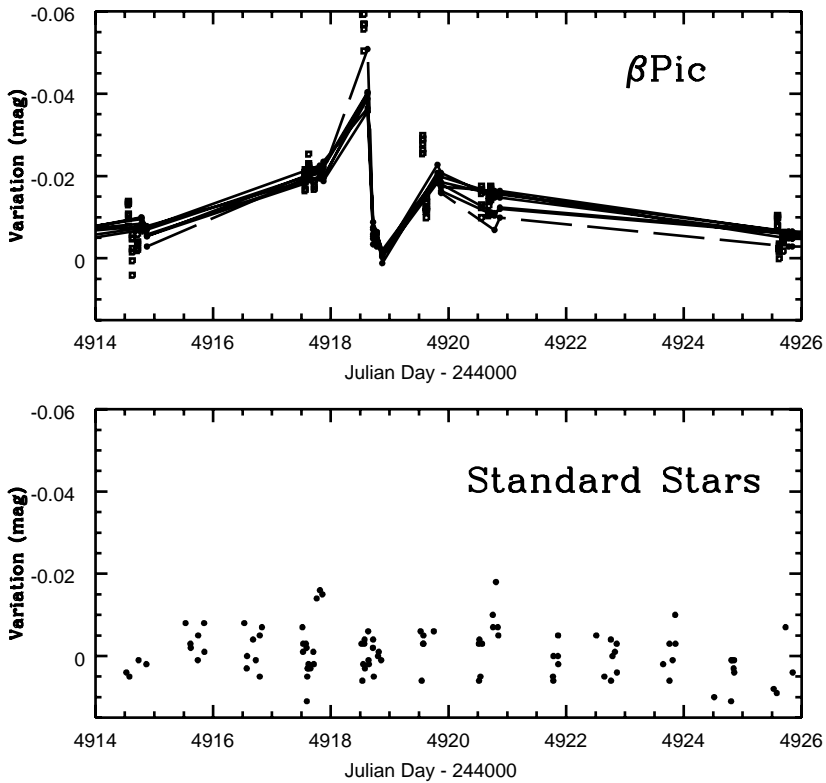


Figure 7 *Top panel:* Photometric variations of  $\beta$  Pic observed within several days of Nov 11, 1981 (JD = 4919). In all seven colors in which the star was monitored (*dots connected by seven solid lines*), the star brightened, returned to roughly undisturbed level, and then brightened again. *Bottom panel:* During the same 12 days, the comparison stars did not show unusual changes. Their colors fluctuated by the small amount indicated by the dispersion shown in the figure, which demonstrates the reality of the  $\beta$  Pic activity. (Courtesy of A Lecavelier des Etangs.)

raises many questions. For instance, why would the brightening match the subsequent occultation; why is the required occulting area so large (about four times the maximum area of any planet or brown dwarf)? Why is the predicted brightening higher than theoretically possible based on the knowledge of dust density in the disk? It is easy to show from Equation 1 that even a complete evacuation of any region in the  $\beta$  Pic disk equal to Jupiter's Roche lobe does not provide enough brightening, for example. We do not know the answers to these questions, but the strange event seems real, as evidenced by the lack of variability of control stars (Figure 7, *lower panel*).

IS THE GAP DUE TO A PLANET? The Kuiper disk has a gap with a relatively sharp edge at  $r \sim 40$  AU caused by planetary perturbations of comets (its associated dust is still unobservable). What about the  $\beta$  Pic disk gap, which is of similar radius (section 3.4)? Theoretical calculations of Roques et al (1994) and Lazzaro et al (1994) show the effect a planet might have on a dust disk that is allowed to evolve under the gravitational perturbations of the planet and the Poynting-Robertson (PR) effect. Particles significantly affected by radiation pressure ( $s = 1\text{--}20 \mu\text{m}$ ) are temporarily trapped in outer first-order mean motion resonances (1:2, 2:3, 3:4, etc). This has a damming effect on the inward PR drift and can create a gap inside the planet's orbit. Lazzaro et al (1994) propose that there may be a Uranus-mass planet at  $r \approx 20$  AU. This is an interesting possibility that should be studied further, including more of the relevant physics of the disk (see next section).

WHAT IS CAUSING DISK ASYMMETRIES? Lazzaro et al (1994) have studied the nonaxisymmetric, arc-shaped structures caused by the perturbation from a slightly eccentric planet in a dust disk subject to the PR effect. These often conspicuously asymmetric structures rotate with angular velocities different from that of the planet, but there may be a relative depletion of dust corotating with the planet as well. The results of this interesting study have been widely overinterpreted in applications to  $\beta$  Pic as explaining the disk asymmetries (e.g. Lecavelier et al 1993, 1995, Sicardy 1994; however, Kalas & Jewitt 1995 notice that asymmetries in different parts of the disk would require many different planets). The arc structures and asymmetries disappointingly disappear when (Artymowicz 1994b): (a) a wide range of initial eccentricities is allowed (small particles are born as debris on orbits with  $0 < e < 1$ ), and (b) interparticle collisions are allowed (particles are destroyed quickly). If not planets, what causes the asymmetries discussed in section 3.2 and 3.4? It can be shown that asymmetries involve much more dust area ( $\sim 10^{28} \text{ cm}^2$ ,  $\sim 10^{24} \text{ g}$ ) than can result from a collision of a pair of planetesimals or protoplanets. Contrived modifications of the idea of dust-planet interaction may be possible, in which dust sources rather than dust itself are shepherded by the planet, but would not account for asymmetries  $\gtrsim 25\%$  (Artymowicz 1994b). The origin of asymmetries appears to be a challenging problem (see section 4.3 for one suggested partial solution).

IS THE THE INNER DISK WARPED BY A PLANET? The inclination of the innermost disk reported in section 3.2, if confirmed, will support the planetary hypothesis of Burrows et al (1995). A planet on an inclined orbit acts on a planetesimal or meteoroid in the disk over secular time scales in such a way as if the planet (and the planetesimal) were rotating mutually-inclined rings. Such rings behave like spinning tops: They precess at a rate proportional to the perturbing

mass. The ascending node of the planetesimal orbit precesses with a period equal to  $(r/r_p)^2(4M_*)/(3M_p)$  times its orbital period, where  $M_*$  and  $M_p$  are the star and planet masses. If one Jupiter mass is present at  $r = 5.2$  AU as in the Solar System, then the inner disk region at  $r \sim 40$  AU could thus be effectively forced to wobble around the planet's, rather than the disk's, plane of motion in just 15 Myr. However, it is difficult to prove that the tilt is necessarily due to a planet, rather than to (an admittedly unlikely) primordial inclination of planetesimal orbits.

#### 4. PHYSICAL PROCESSES GOVERNING THE DUST DISK

In this section we consider the most important physical processes in the dust disk of  $\beta$  Pic, and how they require  $\beta$  Pic to be an early planetesimal or planetary system.

##### 4.1 *Radiation Pressure and Radiative Blowout of Grains*

Radiation pressure (several times larger than in the Solar System) plays an important role in the physics of both gas and dust surrounding  $\beta$  Pic. Most neutral and ionized chemical species have a ratio of radiation pressure to gravity  $\beta > 1$ , i.e. are effectively repelled from the star (but may be kept in the disk by collisions with N, O, and H atoms, which are not propelled by radiation). Although this is not observed to lead to an outflow of the stable component of the gas, it may conceivably lead to a slow migration of gas and solids due to a mismatch of their circular orbital velocities and the resultant weak gas drag. This is especially so because small solid particles are affected by radiation pressure. Radiation pressure during the formation epoch may have been instrumental in determining the Fe:Mg ratio of silicates under certain conditions. If, as in standard formation scenarios neglecting radiation pressure, the grains were at least for some time chemically differentiated into Mg-rich and metallic (and/or carbon-rich) fractions, then radiation pressure (enhanced in the pre-main sequence epoch by the abundant near-UV flux) could selectively have removed the most carbonaceous and ferritic grains into the interstellar medium.

Most compact grains with radii below  $s \sim 1 \mu\text{m}$  and realistic compositions are removed from the system because of  $\beta > 1$  (cf Artymowicz 1988). Because the gas:dust ratio is  $\ll 1$ , the radiative blow-out of such grains is not stopped by the weak gas drag. In particular, submicron ISM grains modeled as a fine-grained 1:1 mixture by volume of "astronomical silicate" and graphite (Draine & Lee 1984) are strongly ejected. The two characteristic values of  $\beta$  for spheres made of any material type (also porous, cf Mukai et al 1992) will be denoted as  $\beta_0 = \beta(s \rightarrow 0)$  and  $\beta_{max}$  (maximum  $\beta$ , typically reached by  $s \approx 0.1 \mu\text{m}$  particles). For compact (90% porous) ISM grains, these values are equal:  $\beta_0 = 6.2$

(6.2), and  $\beta_{max} = 12$  (6.8). Also, a pure astronomical silicate (candidate material for grain matrix in the gap region?) exhibits high radiation pressure parameters: Compact (95% porous) grains have  $\beta_0 = 0.78$  (0.78), and  $\beta_{max} = 7.9$  (1.1); particles larger than  $s = 1.8 \mu\text{m}$  ( $17 \mu\text{m}$ ) have  $\beta < 0.5$ . Transparent ice or magnesium silicates are affected less by radiation. A good candidate material for the main disk, compact (or 75% porous),  $\text{Mg}_{0.8}\text{Fe}_{0.2}\text{SiO}_3$  (cf Dorschner et al 1995) has  $\beta_0 = 0.75$  (0.75) and  $\beta_{max} = 4.3$  (1.6). Spherical particles of this silicate larger than  $s = 1.3 \mu\text{m}$  ( $1.8 \mu\text{m}$ ) have  $\beta < 0.5$ , and can be assumed orbitally stable and abundant. This is because grains released from a larger parent body moving in an orbit with eccentricity  $e \ll 1$  can already escape for  $\beta > 0.5(1 - e) \approx 0.5$ , and not only when  $\beta > 1$ . Except for pure ices with  $s \gtrsim 0.1 \mu\text{m}$ , all solid debris smaller than  $\sim 1 \mu\text{m}$  (many  $\mu\text{m}$  if porous) have a large probability of escape from the system on hyperbolic trajectories. Analogous escape, removing a significant fraction of collisional debris from the solar system, is observed as  $\beta$ -meteoroids (Zook & Berg 1975; orbitally stable particles are called  $\alpha$ -meteoroids). These results provide a plausible explanation for the color-neutral light scattering property of grains in the main disk.

#### 4.2 Implications for the Gap Region

In the gap region, one of the two grain models is appropriate. First, the grains may be compact and have an effective size  $s \approx 2 \mu\text{m}$ , in which case they can both stay in orbit around  $\beta$  Pic and produce the observed  $10 \mu\text{m}$  emission. Second, they may be dark and porous, as seems to be required by IR imaging (section 3.4) and then must be driven out of the gap by radiation (because orbitally stable sizes larger than  $2 \mu\text{m}$  are excluded by  $10 \mu\text{m}$  spectroscopy). The second model is demanding but reasonable from the point of view of mass loss. The time scale for orbital removal beyond  $r = 20 \text{ AU}$  is  $\sim 10^2$  years, or  $\sim 10^{-6}$  of the system's maximum age. The estimated mass of the dust in the gap is  $10^{21.5} \text{ g}$  (Aitken et al 1993). Significant mass ( $\sim 10^{27.5} \text{ g} \sim 1M_E$ ) would thus be lost during 100 Myr if the gap material flows out at a steady rate. (However, similar outflow from the main disk is implausible since it would remove more dust during 100 Myr than a planetary system might have; this was one of the original counter-proofs for  $\beta$  Pic as an outflow phenomenon). An interesting prediction of this reasoning is the possible time-variability of the dust distribution inside the gap on a 10 year timescale. The required mass supply to the gap region may be provided by  $10^6 n_1$  of 1-km-radius evaporating comets, where  $n_1$  is the number of orbital time scales ( $10^2 \text{ year}$ ) each comet survives within the gap before shedding all its dust. The gap region could then be called, borrowing from the title of a recent paper, "a gigantic multi-cometary tail" (Lecavelier et al 1995, cf also Greenberg & Li 1996). (However, the whole disk is too massive to be resupplied by thermal evaporation of comets only, as will follow from section 4.5.)

### 4.3 *Nature vs Nurture in the Interstellar Medium*

Radiation pressure has an important bearing on the issue of internal vs external factors that control the evolution and observability of  $\beta$  Pic and other Vega-type systems. The flux of ISM grains bombarding the circumstellar disk is the chief external factor, depending sensitively on the relative velocity of the star with respect to the ISM. If unimpeded ISM dust flux was present either now or within the very recent past (the past few Myr) then one of two somewhat opposite views might be justified. Lissauer & Griffith (1989) proposed that “sandblasting” by interstellar dust in atomic gas clouds erodes the disks significantly, and that the prominent disk of  $\beta$  Pic might have been saved from significant depletion by virtue of its slow motion with respect to the circular motion in the Galaxy, while other Vega-type systems might have been affected by the abrasive and hostile ISM. On the other hand, Whitmire et al (1992) have proposed that the most prominent examples of the Vega phenomenon are exactly those stars that were recently affected by ISM erosion that has led to the increase of the integrated dust area and visibility. However, Artymowicz (1994) noticed that sandblasting by the ISM may not be effective at all, because typical interstellar grains are smaller than  $1\ \mu\text{m}$ , at which size they are strongly repelled by radiation of the A-type Vega stars. For instance, around  $\beta$  Pic such grains have  $\beta \sim 10$  and do not approach the star (with initial velocity  $8\ \text{km/s}$  at infinity, typical of ISM clouds, and larger than the  $3\text{-km/s}$  velocity of  $\beta$  Pic relative to Galaxy) closer than to within  $\sim 250\text{--}500\ \text{AU}$ , i.e. cannot enter the observed dense disk region. The interesting possibility of large ISM grains entering the disk and generating its slight outer asymmetries is yet to be verified. Such grains are present in our Solar System (Grün et al 1994) but their flux is much too weak compared with the internal particle flux within the  $\beta$  Pic disk to control the evolution of dust.

### 4.4 *Collisions: Creating and Destroying the Dust*

Several processes may alter and move grains in the  $\beta$  Pic disk. In general, they downgrade and destroy the grains in a collisional cascade of sizes analogous to that found in the meteoritic complex of the Solar System (Grün et al 1985). All grain growth processes such as collisional accumulation (snowballing, sticking) and gas accretion can be readily shown to be unimportant. Substantial gas accretion would require time much longer than the collisional time even if unit sticking coefficient is assumed, because (except perhaps in the innermost  $\sim 1\ \text{AU}$  region) the gas:dust flux ratio is  $\ll 1$ . Kinematics of the disk prevent any grain build-up by collisions. Encounter speeds following from vertical motion,  $(z/r)v_K$ , where  $v_K \approx 38(r/\text{AU})^{-1/2}\ \text{km/s}$  is the Keplerian circular velocity, and  $z/r \approx 0.1$ , are certain to lead to net erosion, which starts at less than  $0.1\ \text{km/s}$ .

It is interesting to find the removal time due to the Poynting-Robertson (PR) effect, because this process is at its maximum for observed grain sizes near

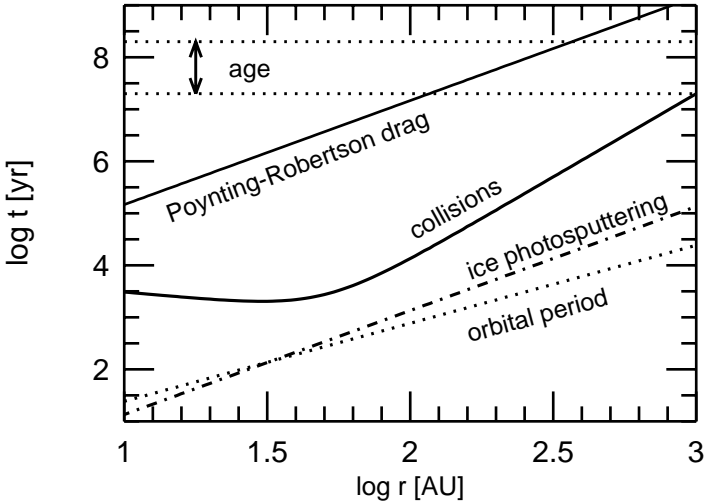


Figure 8 Different destruction and/or removal time scales for a typical dust grain in the  $\beta$  Pic disk, calculated as a function of orbital distance. The collisional time scale is calculated using Equations 1 and 2. The system's age of 20–200 Myr is shown for comparison.

the blow-out limit. For a naive estimate we assume that the disk consists of grains with one typical radius  $s$  and radiation pressure coefficient  $\beta = 1/4$  (near the blow-out limit). The time scale for PR drift toward the star equals (e.g. Roques et al. 1995)  $t_{\text{PR}} = 945(r/\text{AU})^2$  year for a circular initial orbit, and  $t_{\text{PR}} = 1470(r/\text{AU})^2$  year for an initial orbit with eccentricity  $e = \beta/(1 - \beta) = 1/3$  (assuming circular orbit of a parent meteoroid, and small ejection velocity). The second time scale is presented in the log-log plot in Figure 8.

Much of the observed dust originates and is destroyed in collisions. The collisional time  $t_{\text{coll}}$  can be estimated adopting the same values of  $\beta = 1/4$  and  $e = 1/3$  as above. It follows that  $s = 4 \mu\text{m}$  yields the required  $\beta$  for both ice and 75%-porous silicates. The geometric cross section for collision is equal to  $4\pi s^2$ . Typical grains with  $e = 0$  and (average) inclination  $i = 7^\circ$  would undergo collision with probability  $\tau(r)$  per one orbital period  $P$ . The effective optical thickness is roughly  $\sqrt{1 + e^2/i^2} \approx 3$  times larger in case of  $e = 0.33$  and  $i = 0.12$ . The collisional time in our naive derivation reads

$$t_{\text{coll}} \simeq \frac{P}{12\tau}, \quad (2)$$

where  $P = 0.77(r/\text{AU})^{3/2}$  year and  $\tau$  is given by Equation 1. This collisional time scale is as short as several thousand years in the  $r < r_m = 50$  AU region;



much shorter than the PR drift time, as can be seen in Figure 8. Thus the Poynting-Robertson effect is largely irrelevant to  $\beta$  Pic disk.

The naive approximation assumes that two colliding grains break into submicronic fragments upon collision and are lost from the system. The disk is eroded at the rate  $dM_{\text{disk}}/dt = 2 \int dM/t_{\text{coll}}$ , where  $dM$  is the mass of disk element treated as target,  $t_{\text{coll}}$  is the local collisional time, and the factor of 2 reflects the destruction of two equal grains (target and projectile). Using the disk model described by Equations 1 and 2, we obtain  $dM_{\text{disk}}/dt = 2.3 \times 10^{-6} M_E/\text{yr}$ , which corresponds to the destruction of the estimated total mass of solids ( $\sim 120 M_E$ ) in  $t_{120} = 52$  Myr, a value consistent with just one lifetime of the system! This important estimate suggests that the  $\beta$  Pic disk may be eroded at a very fast, in fact, at the maximum achievable rate by grain-grain collisions. Clearly, a more accurate evaluation of disk half-life than that given above is necessary.

#### 4.5 Dust Avalanches and Disk Erosion Rate

Such a calculation has recently been done (P Artymowicz, in preparation) taking into account the grain size distribution of projectiles, targets and debris, orbital element and encounter velocity dispersions, material properties (especially fragmentation strength) from laboratory measurements, incomplete fragmentation, incomplete blowout of debris, and the possibility of so-called dust avalanches in the disk (Artymowicz 1996). The phenomenon of avalanches or chain reaction of outflowing debris striking disk particles and, thereby, creating even more outflowing debris is powered by the radiative energy of the star. It depends critically on the absence of a strong gas drag that would prevent any fast outflows in a gas-dominated protostellar or T Tauri disk. Suppose that  $N_\beta$  submicronic debris is created in a single (erosive or catastrophic) collision between two particles at a distance  $r_0$  from the star (we take  $r_0 < r_m$  initially). The debris is accelerated over a short distance to the final speed  $(\beta - 0.5)v_K(r_0)$ , typically exceeding Keplerian speed  $v_K$  at the collision site. A small percentage of debris, given by the optical thickness of the disk in its midplane, will collide with the disk on its way out at a speed that is more than sufficient to fragment/erode the target disk particles and create further (secondary) debris. For illustration, assume that  $N_\beta = \text{const}$ . Then the flux of debris at infinity depends on  $\tau_\perp$ , and on the covering factor  $\tau_{\text{dust}}$  of the dust as seen from the star exponentially, as  $dM_{\text{disk}}/dt \sim \exp(N_\beta \tau_\perp)$  or  $dM_{\text{disk}}/dt \sim \exp[N_\beta \tau_{\text{dust}}(z/r)^{-1}]$ .

OVERALL EROSION RATE: PLANETARY SYSTEM IN DANGER OF DESTRUCTION? The detailed calculations assuming silicate grain compositions of different porosities show that in  $\beta$  Pic the mass loss is only about 1.7 times larger than that following from disk-disk particle collisions alone; i.e. the proliferation of debris is important but not in the strongly exponential regime. Collisions destroy

the dust-and-sand disk at a rate of  $120 M_E$  per  $t_{120} \sim 90$  Myr. Again, here as in the case of the naive estimate, the disk self-destructs in a time comparable with its estimated age. But if the dustiness<sup>6</sup> was twice its actual value (two times  $\tau_{\text{dust}} = L_{\text{IR}}/L_* = 2.4 \times 10^{-3}$ ), then  $t_{120}$  would sharply drop to 13 Myr, a value about three times shorter than that neglecting the avalanching. Such a destruction time is already uncomfortably short compared with the system's age, and becomes incompatible with the main-sequence status of the star if we attempt to imagine a disk with triple the amount of dust of  $\beta$  Pic ( $t_{120} = 1$  Myr, avalanche enhancement factor 4.6). In conclusion,  $\beta$  Pic in its current configuration is about as dusty as possible given its likely age of several dozen to 100 Myr (see below for further discussion of this point). This is probably an indication of youth, the signature of the clearing period through which planetary systems pass after formation.

The most important point of the theoretical calculations of the kind just described is perhaps the conclusion that the "internal sandblasting" within the  $\beta$  Pic disk is extremely efficient and requires a large reservoir of mass (in the form of large bodies) for continuous erosion. This mass equals or exceeds the mass of solids in the Solar System. The  $\beta$  Pic disk represents either a planetary system or, at a very minimum, a failed Solar System filled with planetesimals in the "isolation" stage (section 2.5) that do not undergo mutual collisions frequently enough to build planets during the main-sequence lifetime of the star.

HOW MANY PLANETESIMALS ARE NECESSARY FOR DUST PRODUCTION? We have seen that avalanches are exponentially strong when the disk density is sufficiently large, but exponentially weak and unimportant when the disk has very small optical depth (smaller than  $\beta$  Pic). In this case, mass loss is proportional to disk density and the collision rate, hence  $dM_{\text{disk}}/dt \sim M_{\text{dust}}^2 \sim \tau_{\text{dust}}^2$ , where  $M_{\text{dust}}$  is the total dust mass. If, in turn, the disk is so sparsely populated ( $\lesssim \text{ZL}$  disk) that the Poynting-Robertson effect takes over the task of removing the grains, then  $dM_{\text{disk}}/dt \sim M_{\text{dust}} \sim \tau_{\text{dust}}$ .

Luu (1994) and Backman et al (1995) estimated the steady-state amount of dust produced by the collisional erosion (cratering) of comets in the Kuiper disk and removed by the Poynting-Robertson effect. They have concluded that the mass and infrared luminosity of Kuiper disk dust (grains with size  $< 0.1$  mm) is a factor  $\sim 10^{-4}$  times that in the  $\beta$  Pic disk (similar to ZL disk). Obviously, the  $\beta$  Pic disk is not an extrasolar Kuiper disk but a more substantial disk of planetesimals. How many of them exactly? Backman et al (1995) used the quadratic dependence of dustiness on the number of parent large bodies to infer that a hundred times more massive Kuiper belt (total of  $\sim 30 M_E$ ) could sustain

<sup>6</sup>Dustiness can be quantitatively defined as the dust-covering factor or the infrared excess divided by the stellar luminosity.

a dust disk as prominent as  $\beta$  Pic disk. In fact, even more mass is needed in the density regime  $\beta$  Pic operates in, where the quadratic dependence just mentioned becomes linear, as a consequence of the dust-collisional time scale replacing the P-R time scale. It can be shown that in a steady state, the total mass of planetesimals in the  $\beta$  Pic disk is approximately equal to the total dust mass times the square root of the ratio of planetesimal to dust radius (times a factor of order 1.5 due to kinematical differences between dust and planetesimals). For  $M_{\text{dust}} = 10^{25.5}$  g,  $4 \mu\text{m}$ -sized grains, and 1-km planetesimals, planetesimal mass  $\approx 125 M_Z$  is obtained, in excellent agreement with the estimate based on the theory of planetary systems (section 2). Again we see that the full mass of a planetary system like our own (but in the planetesimal stage) is necessary to explain the observations.

#### 4.6 *Can the Dust Be Icy?*

In section 2.2 we mentioned that water ice is expected to comprise about one quarter of the mass of planetesimals. Other less stable ices ( $\text{CO}_2$ ,  $\text{NH}_3$ ,  $\text{CH}_4$ ) may be present at the  $\sim 10\%$  level. The icy composition of dust released from such planetesimals and their fragments would naturally explain why  $\beta$  Pic and most other Vega systems have central gaps where grain temperature would otherwise exceed 120–150 K (limit of water ice sublimation). The white or gray color and high reflectivity of slightly dirty ices are consistent with models of the main disk. However, no spectroscopic evidence has been found to date for an icy composition of the dust. This is not surprising, at least according to the following theoretical considerations.

**PHOTOEVAPORATION OF ICES** The first serious problem with an icy composition for grains around Vega-type stars is the rapid ice destruction by non-thermal photosputtering, not only in the gap region (thermal evaporation) but throughout the disk. As discussed by Artymowicz (1994a), this process can be conceptually divided into photodesorption (also known as photoevaporation, photodetachment) when the surface layer of  $\text{H}_2\text{O}$  molecules absorb stellar UV photons and are excited into a repulsive electronic state leading to ejection, and photolysis (photodissociation) when the molecule is ejected in pieces. In the Solar System, these processes are  $\sim 10^3$  times less efficient than in  $\beta$  Pic owing to the weak solar UV flux between approximately  $1500 \text{ \AA}$  and  $1700 \text{ \AA}$ . A new evaluation of the rate of size decrease due to photosputtering by  $\beta$  Pic yields a value  $\dot{s} \approx -30(r/\text{AU})^{-2} \mu\text{m}/\text{yr}$ , assuming that one half of the grain surface is covered by pure ice (Artymowicz 1996). The destruction time of  $s = 4 \mu\text{m}$  grains is plotted as a function of radius in Figure 8. It is comparable with orbital periods throughout most of the disk, and much shorter than collisional times of grains. Clearly, this appears to preclude the possibility that  $\beta$  Pic grains have

fresh ice on their surface. Not only would the total photoevaporation rate of the disk then become too high ( $120 M_E$  in just 4 Myr), but also an unobserved dense water vapor cloud would surround the star. An ad hoc hypothesis aimed at saving the icy options can be considered, in which the interior of the icy grain contains a very finely grained silicate component that somehow remains and accumulates on the grain surface to form a thin crust shielding the grain from direct UV radiation (“micro-cometary” grain model). However, this possibility seems speculative as, unlike comets, dust grains do not have sufficient gravity to cause accumulation of a shielding crust or regolith.

**MECHANICAL BREAKUP OF ICES** The second, equally serious, problem with the icy dust composition in  $\beta$  Pic is the brittle mechanical structure of ice, which makes an icy grain break into thousands of pieces in any high-velocity collision with another grain. If the fragmentation strength of ice rather than pure silicate (material much closer mechanically to diamond than ice) is used in detailed collisional calculations of the disk, then dust avalanches are so strong that a single collision of two planetesimals in the inner disk could lead to the immediate destruction of a large section of a disk. In conclusion, theory suggests that icy planetesimals collide and break into gradually smaller and ice-poor fragments, and that the observed dust is entirely ice-free.

**GRAINS FROM EVAPORATED COMETS OR CRATERED ASTEROIDS?** It is not yet clear whether most of the interplanetary dust complex in the inner Solar System is resupplied by asteroid collisions or thermal evaporation of comets (Leinert et al 1983, Levasseur-Regourd et al 1990, 1991, Gustafson 1994). These two supply mechanisms could be equally important to within an order of magnitude. The situation in  $\beta$  Pic is even less clear at the moment. Greenberg & Li (1996) and Lecavelier et al (1996) proposed that grain release due to thermal evaporation of cometary ices resupplies the whole disk in siliceous dust with the help of radiation pressure. The idea is appealing and consistent with the presence of FEBs. However, it encounters a quantitative difficulty of resupplying the dust at the large total rate of  $\sim 1 M_E$  per Myr that is required (as opposed to a much smaller rate required to replenish the gap region; cf section 3.5). This is a problem unless the ice contains a much larger fraction of  $\text{CO}_2$  and more volatile compounds than are found in Solar System comets, such that the ice sublimates at distances of order 100 AU from the star (for instance,  $\text{CO}_2$  sublimates at a three times larger distance than  $\text{H}_2\text{O}$ ). We should also note that typical  $\beta$  Pic grains are in some ways different from cometary dust as we know it (cf section 3.7). It remains to be seen if non-thermal release mechanisms (like photosputtering), or simply microcratering and meteoroid collisions are sufficient for dust generation.

#### 4.7 *Is $\beta$ Pic Unique or Typical?*

For an entire past decade, one of the most puzzling facts about Vega-type stars has been our inability to find other examples of disks that scatter starlight and can be directly seen in the visible bands, despite attempts directed at imaging the surroundings of hundreds of nearby stars known to emit a thermal IR excess (cf Backman & Paresce 1993, Kalas & Jewitt 1996). There are many possible reasons why other stars avoid detection in this way: intermediate or pole-on viewing geometry, larger distance, darker grains. Whereas some of these reasons may be correct, none can satisfactorily explain why  $\beta$  Pic is also so prominent in the infrared spectrum. Other similar systems, if they existed, could have been easily detected by IRAS out to a considerable distance. This raises suspicion that  $\beta$  Pic is somehow very unique.

On the observational side, resolution of this issue begins with new spatially resolved mid-IR imaging of the Vega-type system SAO 26804 by Skinner et al (1995), which includes a disk viewed at an intermediate inclination. Perhaps such disks will soon be detected in scattered light. Theoretical aspects of the uniqueness issue were addressed by Artymowicz (1996), who demonstrated that Vega-type systems have a bimodal distribution of dustiness ( $\tau_{dust} = L_{IR}/L_*$ ): One group has  $\tau_{dust} \leq 2.4 \times 10^{-3}$  (that of  $\beta$  Pic), the other typically  $10^2$  times larger IR excesses. He proposed that  $\beta$  Pic is the most dusty gas-poor system of its class because it is close to the theoretical-limiting dustiness above which disk erosion (especially the efficient avalanche activity) destroys the dust and the parent bodies in a very short time ( $<1$  Myr). The remaining high-dustiness systems must therefore be much younger (T Tau or post-T Tau stars still embedded in their solar nebulae) and gas-rich, to prevent the high grain-grain impact velocities leading to dust self-destruction and blowout. According to this theory,  $\beta$  Pic is unique only in the sense that it is extremely dusty and therefore a relatively young main-sequence star. According to mass-loss rates discussed in section 4.5, it will likely become less dusty and more visually similar to other stars of its class as well as the Solar System within the time  $t \sim t_{120} \approx 100$  Myr. Moreover, because the grinding rate and dustiness following the loss of the primordial nebula were once higher, we are led to the conclusion that the timescale  $t_{120} \sim 100$  Myr yields a rather strict upper limit on the disk's age (counted from the disappearance of primordial gas), while the actual age may be a few times shorter. However, the disk cannot be very young because one would expect there to have been a significant depletion of rock-forming refractory elements in the star's atmosphere following the final accretion of nebular gas devoid of elements that remained in orbit to form the dusty disk (cf Artymowicz 1996). Still, there is little evidence of any current depletion (in other words,  $\beta$  Pic is not a  $\lambda$  Boo star; Holweger & Rentsch-Holm 1995),

which suggests that enough time ( $>10$  Myr?) has passed since the nebula dispersal to allow meridional stellar circulation to mix the metal-poor veneer of gas with the stellar interior.

Other  $\beta$  Pic stars are hard to find because their collisional (and gravitational?) clearing proceeds so fast that they are outnumbered by more advanced, slowly evolving, and less dusty systems (most of low-dustiness Vega-type stars). In this context, the Sun's clearing epoch, which lasted up to 800 Myr, may appear atypically long. But as mentioned before, we do not know if and for how long the Solar System's gas-free dust disk resembled that of  $\beta$  Pic, and a basic similarity is not excluded.

We thus arrive at the conclusion that  $\beta$  Pic most likely is a young solar-like system that formed and then shortly thereafter lost its primordial gaseous disk 20–100 Myr ago.

## 5. BETA PICTORIS VS SOLAR SYSTEM

Exactly how “solar” a system is  $\beta$  Pic? What are the largest bodies circling around the star? While there is much potential for a system like  $\beta$  Pic (with its numerous planetesimals) to form planets, the question of whether planets are or will be formed within the next billion years (the star's life span) remains a fascinating and unresolved issue. The discovery of extrasolar planets discussed in the introduction certainly suggests that the presence of planets is a strong possibility and motivates a careful search for them around  $\beta$  Pic. Meanwhile, the most concrete comparisons we have, discussed throughout the paper and briefly summarized in this section, deal mostly with observable dust and planetesimals.

### 5.1 *Similarities with the Solar System*

1. The dust-dominated, geometrically thin disk with opening angle of order  $10^\circ$  surrounding  $\beta$  Pic fits well with the theoretical expectations of a similar structure in a young planetary system that has lost its primordial protostellar/protoplanetary gas.
2. As in our planetary system, the dust component of  $\beta$  Pic must be replenished on a time scale much shorter (typically  $10^4$  year) than the system's age (likely in the range 20–100 Myr), and by the same mechanisms (collisions of larger particles, evaporation and/or photosputtering of icy parent bodies). The parent bodies (small planetesimals) must have a combined mass of roughly  $\sim 125$  Earth masses in order to maintain the observed dust disk in a quasi-steady state. This mass agrees with the theoretically-expected mass of solid bodies in a planetary system,  $\approx 120 \pm 40$  Earth masses.

3. A young planetary system is thought to undergo a clearing period (epoch of giant impacts) lasting a few hundred million years, during which its dust and meteoroid population (but not the total mass) is several orders of magnitude larger than in the present Solar System. The collisional grinding rate and characteristic dust mass  $\sim 10^4$  times that in the Solar System are more than sufficient to fulfill that expectation. In fact, calculations show that  $\beta$  Pic is nearly as dusty as possible without leading to a paradox of self-destruction on time scales of  $\gtrsim 1$  Myr.
4. The dust of  $\beta$  Pic has a wide size distribution with most area contributed by 1–10  $\mu\text{m}$  particles that have neutral-grey scattering and high albedo ( $A \gtrsim 0.4$ ). These optical properties make it similar in the broad outline to the interplanetary (zodiacal light) particles in our Solar System. The linear polarization ( $17 \pm 3\%$ ), with electric field aligned with the disk rotational axis, is very similar to that of zodiacal light.
5. The dust of  $\beta$  Pic has a composition similar to common Solar System materials. Spectroscopy of the 10  $\mu\text{m}$  emission feature shows that the warm dust present in the central gap region consists mainly of amorphous silicates, with the addition of crystalline olivine, very similar to the dust of comet Halley, perhaps even sharing the same thermal processing history that led to crystallization. Although the main disk probably consists of different, brighter, and less carbonaceous and/or Fe-rich grains (see below), its properties are similar to Mg-rich olivines and pyroxenes which, taken together, are thought to be the single most common solid material in planetary systems.
6. There is neither observational nor theoretical evidence that  $\beta$  Pic dust might have a volatile (icy) composition, the same being true of the interplanetary dust in our system.
7. Both  $\beta$ -meteoroids and  $\alpha$ -meteoroids are present in  $\beta$  Pic, i.e. grains strongly/weakly affected by radiation pressure.
8. The size distribution of solid particles extends to macroscopic bodies. Millimeter-wavelength observations already detect sand (mm-sized bodies), and the total observed mass (almost an Earth mass) is contained in the largest observed bodies.
9. Episodic spectroscopic “accretion events” caused  $\sim 10^2$  times per year by planetesimals (most likely analogous to small Solar System comets and/or their orbital families) provide a strong link to the young Solar System, where  $10^{14}$  such bodies formed and mostly accumulated into planets. The evaporated and ionized gas released by planetesimals close to the star has a solar chemical abundance pattern.

10. Moon-size ( $10^3$  km) objects may be present throughout the disk to provide gravitational “stirring” that helps establish the observed finite thickness of the disk.
12. Although still conjectural, planet(s) may be present or forming in the  $\beta$  Pic system. (Terrestrial planets in our system formed in a time comparable with the estimated age of  $\beta$  Pic.) Their presence could help explain the inner clearing region in the dust disk ( $r \lesssim 40$  AU, similar to the inner void in the Kuiper disk of comets), and the newly claimed warp in the  $r = 40 - 100$  AU region. Planets (at least Moon-sized objects) may gravitationally redirect the planetesimals toward the star (causing the Falling Evaporating Bodies), as well as place some bodies on elongated orbits in the analogue of Oort cloud of comets. Less likely is the possibility that planets might also be involved in creating the observed disk asymmetries.

## 5.2 *Dissimilarities with the Solar System*

1. The large radial extent of the disk (much larger than the canonical radius of protoplanetary disks  $\sim 100$  AU) has been a mild surprise, but may not be a serious issue if the outer disk material originated within a smaller radius and was later displaced by gravitation and radiation. (We tend to favor such a scenario because we do not fully understand the formation and evolution of planetesimals at radii as large as 1000 AU from the star.)
2. The bulk of the  $\beta$  Pic grains may be somewhat different than the typical (current) Solar System interplanetary and cometary material. The albedo is probably higher, color more neutral (less red in the visible range), and hence the inferred Fe:Mg ratio and C content smaller (e.g. Fe:Mg  $\lesssim 0.3$ ) than in both the canonical chondritic composition (Fe:Mg  $\approx 0.8$ ) and the carbonaceous meteoroids and micrometeoroids (often Fe:Mg  $\sim 0.4$ ), especially the dark cometary dust. (Incidentally, typical  $\beta$  Pic dust is clearly different, both chemically and in size, from unprocessed interstellar dust, which strengthens its ties with planetary materials).
3. In the Solar System, ZL particles exhibit a mild trend of larger albedo at a smaller heliocentric distance, whereas in  $\beta$  Pic no such trend has been seen. To the contrary, darker (hotter) cometary-like grains might be present in the inner gap region, and brighter (less Fe and C-rich) grains outside the gap.
4. The size distribution of dust may include more  $\mu\text{m}$ -sized grains in  $\beta$  Pic than in the zodiacal light (dominated by 10–100  $\mu\text{m}$  grains). However, strictly speaking, we do not know if there is any substantial dissimilarity with today’s or, especially, the early Solar System.



5. The role of radiation pressure acting on both grains and many gas species is larger in  $\beta$  Pic than in our system. Qualitative differences caused by that pressure (and by large dustiness) include the possibility of dust avalanches of submicron-sized collisional debris streaming outward through the disk. The Poynting-Robertson drift, instrumental in cleaning the Solar System of dust by transporting it toward the Sun, is superseded in  $\beta$  Pic by the much more rapid collisional disruption of dust followed by outward removal of fragments by radiation pressure. In our system, only certain size intervals are colliding before substantially drifting in. The higher mass of the star and larger radiation-induced eccentricities make grain collisions more disruptive in  $\beta$  Pic.
6. The interplanetary environment is different. As an A-type star,  $\beta$  Pic is not expected to have much chromospheric or coronal activity and should have no solar wind with strong magnetic fields. But the stellar UV flux is much stronger in  $\beta$  Pic, and the photosputtering thus destroys surfaces covered with ice much faster than in the Solar System.
7. Our zodiacal cloud has only slight asymmetries and distortions, but nothing as spectacular as seen in Figure 3. It contains  $\sim 10^4$  times less dust, distributed in a disk a few times thicker than the  $\beta$  Pic disk.

### 5.3 Conclusions

A decade ago one could wonder about which observation would be the more interesting and informative: the discovery of a planet in a well-established orbit around a normal star, or the discovery of a somewhat messy planetary system caught during formation, with lots of dust and yet unclear signatures of finished planets. Now, as then, the preference is not obvious because both types of discoveries can provide us with important and complementary insights. For instance, although it may be very difficult to derive an accurate orbit for a planet from the observed distribution of dust and sand around it, chemical and mineralogical questions are best addressed with such direct spectroscopic observations.

We were very fortunate to witness the discovery of both young and old planetary systems (see section 1),  $\beta$  Pic being the first young one to have been explored in some detail. Importantly, we know that the extrasolar systems are not unique in the universe but fairly common, even if only  $\sim 5\%$  of all solar-type stars may harbor giant planets. Young systems such as  $\beta$  Pic are rare in the sky, because their youth (epoch of large dustiness) is brief (Section 4.7). Nevertheless, they exemplify a common early phase in the lives of many and perhaps most stars. Further study of the  $\beta$  Pic disk will hopefully solve

its remaining mysteries (most nagging at present is perhaps the origin of disk asymmetries and the existence of planets), improve our understanding of its connections with the early Solar System, and eventually provide us with a convenient, nearby (by cosmic standards) laboratory for testing our concepts of planetary system formation and evolution. Such exploration should be guided by the extensive knowledge about the Solar System, and vice versa.

#### ACKNOWLEDGMENTS

It is a pleasure to thank all those who have been sending me their results and offering informative discussions, particularly the following: Dana Backman, Herve Beust, Chris Burrows, Mark Clampin, Sergio Fajardo-Acosta, Paul Kalas, Roger Knacke, Pierre-Olivier Lagage, Anne-Marie Lagrange, Alain Lecavelier des Etangs, Eric Pantin, Francesco Paresce, and Alfred Vidal-Madjar. Dana Backman's thorough reading of the manuscript and many suggested corrections were extremely helpful. Support by a research grant from NFR (Swedish Natural Science Research Council) and the Visitor Program at Space Telescope Science Institute in Baltimore is also gratefully acknowledged.

Visit the *Annual Reviews* home page at  
<http://www.annurev.org>.

#### Literature Cited

- Aitken DK, Moore TJT, Roche PE, Smith CH, Wright CM. 1993. Mid-infrared spectroscopy of Beta Pictoris—constraints on the dust grain size. *Mon. Not. R. Astron. Soc.* 265:L41–43
- Artymowicz P. 1988. Radiation pressure forces on particles in the Beta Pictoris system. *Astrophys. J. Lett.* 335:L79–82
- Artymowicz P. 1992. Dynamics of binary and planetary-system interaction with disks: eccentricity changes. *Publ. Astron. Soc. Pacific* 104:769–74
- Artymowicz P. 1994a. Modeling and understanding the dust around Beta Pictoris. See Ferlet & Vidal-Madjar 1994, pp. 47–65
- Artymowicz P. 1994b. Planetary hypothesis and the asymmetries in the Beta Pictoris disk. See Ferlet & Vidal-Madjar 1994, pp. 335–37
- Artymowicz P. 1996. Vega-type systems. See U Käüfl & R Siebenmorgen 1996, pp. 137–48
- Artymowicz P, Burrows C, Paresce F. 1989. The structure of the Beta Pictoris circumstellar disk from combined IRAS and coronographic observations. *Astrophys. J.* 337:494–513
- Artymowicz P, Lubow SH. 1996. Mass flow through gaps in circumbinary disks. *Astrophys. J. Lett.* 467:L77–L80
- Artymowicz P, Paresce F, Burrows C. 1990. The structure of the Beta Pictoris disk and the properties of its particles. *Adv. Space Res.* 10(3):81–84
- Aumann HH. 1988. Spectral class distribution of circumstellar material in main-sequence stars. *Astron. J.* 96:1415–19
- Aumann HH, Good JC. 1990. *Astrophys. J.* 350:408–12
- Backman DE, Dasgupta A, Stencel RE. 1995. Model of a Kuiper belt small grain population and resulting far-infrared emission. *Astrophys. J. Lett.* 450:L35–38
- Backman DE, Gillett FC, Witteborn FC. 1992. Infrared observations and thermal models of the  $\beta$  Pictoris dust disk. *Astrophys. J.* 385:670–79
- Backman DE, Paresce F, eds. 1993. Main-sequence stars with circumstellar solid material: the Vega phenomenon. See Levy et al 1993, pp. 1253–304
- Beust H. 1994.  $\beta$  Pictoris: The “Falling Evaporating Bodies” model. See Ferlet & Vidal-Madjar 1994, pp. 35–46

- Beust H, Vidal-Madjar A, Ferlet R, Lagrange-Henri AM. 1994. Cometary-like bodies in the protoplanetary disk around  $\beta$  Pictoris. *Astrophys. Space Sci.* 212:147–57
- Beust H, Morbidelli A. 1996. Mean motion resonances as a source for infalling comets toward  $\beta$  Pictoris. *Icarus* 120:358–70
- Blanco A, Orfino V, Bussoletti E, Fonti S, Colangeli L, et al. 1991. Laboratory spectra of amorphous and crystalline olivine: an application to comet Halley IR spectrum. See Levasseur-Regourd & Hasegawa 1991, pp. 125–28
- Boggess A, Bruhweiler FC, Grady CA, Ebbets DC, Kondo Y, et al. 1991. First results from the Goddard high-resolution spectrograph: resolved velocity and density structure in the Beta Pictoris circumstellar gas. *Astrophys. J. Lett.* 377:L49–52
- Bradley JP, Sanford, SA, Walker RM. 1988. Interplanetary dust particles. In *Meteorites and the Early Solar System*, ed. JF Kerridge, MS Matthews. Tucson: Univ. Ariz. Press. pp. 861–95
- Bregman JD, Witteborn FC, Allamandola LJ, Campins H, Wooden DH, et al. 1987. Airborne and groundbased spectrophotometry of comet P/Halley from 5–13 micrometers. *Astron. Astrophys.* 187:616–20
- Bruhweiler FC, Grady CA, Kondo Y. 1991. Mass outflow in the nearby proto-planetary system, Beta Pictoris. *Astrophys. J. Lett.* 371:L27–31
- Burrows C, Krist JE, Stapelfeldt KR, WFPC2 Investigation Team. 1995. HST observations of the Beta Pictoris Circumstellar Disk. *Bull. Am. Astron. Soc.* 187:#32.05 (Abstract.)
- Butler RP, Marcy GW. 1996. A planet orbiting 47 UMa. *Astrophys. J. Lett.* 464:L153–56
- Campins H, Ryan E. 1989. The identification of crystalline olivine in cometary silicates. *Astrophys. J.* 341:1059–66
- Chini R, Krügel E, Kreysa E. 1990. Large dust particles around main sequence stars. *Astron. Astrophys.* 227:L5–8
- Chini R, Krügel E, Shustov B, Tutukov A, Kreysa E. 1991. Dust disks around Vega-type stars. *Astron. Astrophys.* 252:220–28
- Cochran AL, Levison HL, Stern SA, Duncan MJ. 1995. The discovery of Halley-sized Kuiper belt objects using the Hubble Space Telescope. *Astrophys. J.* 455:342–46
- Diner DJ, Appleby JF. 1986. Prospecting for planets in circumstellar dust—sifting the evidence from Beta Pictoris. *Nature* 322:436–38
- Dorschner J, Begemann B, Henning T, Jäger C, Mutschke H. 1995. Steps toward interstellar silicate mineralogy. II. Study of Mg-Fe-silicate glasses of variable composition. *Astron. Astrophys.* 300:503–23
- Draine BT, Lee HM. 1984. Optical properties of interstellar graphite and silicate grains. *Astrophys. J.* 285:89–108
- Duncan MJ, Quinn T. 1993. The long-term dynamical evolution of the solar system. *Annu. Rev. Astron. Astrophys.* 31:265–95
- Ferlet R, Vidal-Madjar A, eds. 1994. *Circumstellar Dust Disks and Planet Formation*. Gif sur Yvette: Éd. Front. 395 pp.
- Gillett FC. 1986. IRAS observations of cool excess around main sequence. In *Light on Dark Matter*, ed. FP Israel, pp. 61–69. Dordrecht: Reidel
- Gledhill TM, Scarrott SM, Wolstencroft RD. 1991. Optical polarization of the disc around  $\beta$  Pictoris. *Mon. Not. R. Astron. Soc.* 252:50P–54P
- Golimowski DA, Durrance ST, Clampin M. 1993. Coronagraphic imaging of the Beta Pictoris circumstellar disk—evidence of changing disk structure within 100 AU. *Astrophys. J. Lett.* 411:L41–44
- Good JC, Hauser MG, Gautier TN. 1986. IRAS observations of the zodiacal background. *Adv. Space Res.* 6(7):83–86
- Greenberg JM, Hage JJ. 1990. From interstellar dust comets: a unification of observational constraints. *Astrophys. J.* 361:260–74
- Greenberg JM, Li A. 1996. Comets as a source of the dust in the  $\beta$  Pictoris disk. See Käuffl & Siebenmorgen 1996, pp. 161–74
- Grün E, Gustafson B, Mann I, Baguhl M, Morfill GE, et al. 1994. Interstellar dust in the heliosphere. *Astron. Astrophys.* 286:915–24
- Grün E, Zook HA, Fechtig H, Giese RH. 1985. Collisional balance of the meteoritic complex. *Icarus* 62:244–72
- Gustafson BAAS. 1994. Physics of zodiacal dust. *Annu. Rev. Earth Planet. Sci.* 22:553–95
- Holweger H, Rentzsch-Holm I. 1995. High-resolution spectroscopy of lambda Bootes stars and “dusty” normal A-stars: circumstellar gas, rotation, and accretion. *Astron. Astrophys.* 303:819–32
- Jewitt D, Luu J. 1993. Discovery of the candidate Kuiper belt object 1992 QB<sub>1</sub>. *Nature* 362:730–32
- Jewitt D, Luu J. 1995. The Solar System beyond Neptune. *Astron. J.* 109:1867–76
- Käuffl HU, Siebenmorgen R, eds. 1996. *The Role of Dust in the Formation of Stars*. Berlin: Springer. 461 pp.
- Kalas P, Jewitt D. 1995. Asymmetries in the Beta Pictoris dust disk. *Astron. J.* 110:794–804
- Kalas P, Jewitt D. 1996. The detectability of beta Pic-like circumstellar disks around nearby main-sequence stars. *Astron. J.* 111:1347–55
- Knacke RF, Fajardo-Acosta SB, Telesco CM, Hackwell JA, Lynch DK, et al. 1993. The

- silicates in the disk of Beta Pictoris. *Astrophys. J.* 418:440–50
- Kondo Y, Bruhweiler FC. 1985. IUE observations of Beta Pictoris— an IRAS candidate for a proto-planetary system. *Astrophys. J. Lett.* 371:L1–5
- Lagage PO, Pantin E. 1994. Dust depletion in the inner disk of Beta Pictoris as a possible indicator of planets. *Nature* 369:628–30
- Lagrange AM. 1994. The Beta Pictoris spectrum: some remaining questions. See Ferlet & Vidal-Madjar 1994, pp. 19–28
- Lagrange AM, Vidal-Madjar A, Deleuil M, Emerich C, Beust H, et al. 1995. The Beta Pictoris circumstellar disk. XVII. Physical and chemical parameters of the disk. *Astron. Astrophys.* 296:499–508
- Lagrange-Henri AM. 1995. Observations of disks around main sequence stars ( $\beta$  Pictoris). *Astroph. Space Sci.* 223:19–43
- Lamy PL, Perrin JM. 1991. The optical properties of interplanetary dust. See Levasseur-Regourd & Hasegawa 1991, pp. 163–70
- Lanz T, Heap SR, Hubeny I. 1995. HST/GHRS observations of the  $\beta$  Pictoris system: basic parameters and the age of the system. *Astrophys. J.* 447:L41–44
- Latham DW, Mazeh T, Stefanik RP, Mayor M, Burki G. 1989. The unseen companion of HD114762: a probable brown dwarf. *Nature* 339:38–40
- Lazzaro D, Sicardy B, Roques F, Greenberg R. 1994. Is there a planet around  $\beta$  Pictoris? Perturbations of a planet on a circumstellar dust disk. 2. The analytical model. *Icarus* 108:59–80
- Lecavelier des Etangs A, Perrin G, Ferlet R, Vidal-Madjar A, et al. 1993. Observations of the central part of the Beta Pictoris disk with an anti-blooming CCD. *Astron. Astrophys.* 274:877–82
- Lecavelier des Etangs A, Deleuil M, Vidal-Madjar A, Ferlet R, Nitschelm C, et al. 1995.  $\beta$  Pictoris: evidence of light variations. *Astron. Astrophys.* 299:557–62
- Lecavelier des Etangs A, Vidal-Madjar A, Ferlet R. 1996. Dust distribution in disks supplied by small bodies: Is the  $\beta$  Pictoris disk a gigantic multi-cometary tail? *Astron. Astrophys.* 307:542–50
- Leinert C, Röser S, Buitrago J. 1983. How to maintain the spatial distribution of interplanetary dust. *Astron. Astrophys.* 118:345–57
- Levasseur-Regourd AC, Dumont R, Renard JB. 1990. A comparison between polarimetric properties of cometary dust and interplanetary particles. *Icarus* 86:264–72
- Levasseur-Regourd AC, Hasegawa H, eds. 1991. *Origin and Evolution of Interplanetary Dust*. Dordrecht: Kluwer. 454 pp.
- Levasseur-Regourd AC, Renard JB, Dumont R. 1991. Dust optical properties—a comparison between cometary and interplanetary grains. *Adv. Space Res.* 11:175–82
- Levison HF, Duncan NJ, Wetherill GW. 1994. Secular resonances and cometary orbits in the beta Pictoris system. *Nature* 372:441–43
- Levy EE, Lunine JJ, Matthews MS, eds. 1993. *Protostars and Planets III*. Tuscon: Univ. Ariz. Press. 1596 pp.
- Lissauer JJ. 1993. Planet formation. *Annu. Rev. Astron. Astrophys.* 31:129–74
- Lissauer JJ, Griffith CA. 1989. Erosion of circumstellar particle disks by interstellar dust. *Astrophys. J.* 340:468–71
- Luu J. 1994. The Kuiper belt and circumstellar disks. See Ferlet & Vidal-Madjar 1994, pp. 195–205
- Marcy GW, Butler RP. 1996a. A planetary companion to 70 Vir. *Astrophys. J. Lett.* 464:L147–51
- Marcy GW, Butler RP. 1996b. Planets around main sequence stars. Invited rev. pap. at *Planetary Formation in the Binary Environment Meet.*, June 16–18, State Univ. New York, Stony Brook
- Mayor M, Queloz D. 1995. A Jupiter-mass companion to a solar-type star. *Nature* 378:355–59
- Mazeh T, Mayor M, Latham DW. 1997. Eccentricity vs. mass for low-mass secondaries and planets. *Astrophys. J.* In press
- McDonnell JAM, Lamy PL, Pankiewicz GS. 1991. Physical properties of cometary dust. In *Comets in the post-Halley era*, ed. RL Newburn, M Neugebauer, J Rahe, 2:1043–73. Dordrecht: Kluwer
- Mouillet D, Lagrange AM. 1995. The Beta Pictoris circumstellar disk. XX. Some physical parameters of the gaseous component. *Astron. Astrophys.* 297:175–82
- Mukai T, Ishimoto H, Kozasa T, Blum J, Greenberg JM. 1992. Radiation pressure forces of fluffy porous grains. *Astron. Astrophys.* 262:315–20
- Nakano T. 1988. Formation of planets around stars of various masses. II. Stars of two and three solar masses and the origin and evolution of circumstellar dust clouds. *Mon. Not. R. Astron. Soc.* 230:551–71
- Ney EP, Merrill KM. 1976. Comet West and the scattering function of cometary dust. *Science* 194:1051–53
- Norman CA, Paresce F. 1989. Circumstellar material around nearby stars: Clues to the formation of planetary systems. See Weaver & Danly 1989, pp. 151–69
- Pantin E. 1996. *Etude de la partie interne du disque de poussières de  $\beta$  Pictoris*. PhD thesis. Saclay: Univ. Paris-Sud. 228 pp.
- Paresce F. 1991. On the evolutionary status of

- Beta Pictoris. *Astron. Astrophys.* 247:L25–28
- Paresce F, Burrows C. 1987. Broad-band imaging of the Beta Pictoris circumstellar disk. *Astrophys. J. Lett.* 319:L23–25
- Prinn RG. 1993. Chemistry and evolution of gaseous circumstellar disk. See Levy, Lunine, & Matthews 1993, pp. 1005–28
- Rietmeijer FJM. 1992. Carbon petrology in cometary dust. In *Asteroids, Comets, Meteors 1991*. Houston: Lunar Planet. Inst. pp. 513–16
- Roques F, Scholl H, Sicardy B, Smith BA. 1994. Is there a planet around  $\beta$  Pictoris? Perturbations of a planet on a circumstellar dust disk. 1. The numerical model. *Icarus* 108:37–58
- Sandford SA. 1991. Constraints on the parent bodies of collected interplanetary dust particles. See Levasseur-Regourd & Hasegawa 1991, pp. 125–28
- Skyles MV, Walker RG. 1992. The nature of comet nuclei. In *Asteroids, Comets, Meteors 1991*. Houston: Lunar Planet. Inst. pp. 587–91
- Smith BA, Terrile RJ. 1984. A circumstellar disk around Beta Pictoris. *Science* 226:1421–24
- Soderblom LA, Condit CA, West RA, Herman BM, Kreidler TJ. 1974. Martian planetwide crater distribution. *Icarus* 22:239–64
- Strom SE, Edwards S, Skrutskie MF. 1993. Evolutionary time scales for circumstellar disks associated with intermediate- and solar-type stars. See Levy, Lunine & Matthews 1993, pp. 836–66
- Telesco CM, Knacke RF. 1991. Detection of silicates in the  $\beta$  Pictoris disk. *Astrophys. J. Lett.* 372:L29–31
- Vidal-Madjar A, Ferlet R. 1994.  $\beta$  Pictoris: the gaseous circumstellar disk. See Ferlet & Vidal-Madjar 1994, pp. 7–17
- Vidal-Madjar A, Lagrange-Henri AM, Feldman PD, Beust H, Lissauer JJ, et al. 1994. HST-GHRS observations of  $\beta$  Pictoris: additional evidence for infalling comets. *Astron. Astrophys.* 290:245–58
- Ward WR. 1986. Density waves in the solar nebula: differential Landblad type. *Icarus.* 67:164–80
- Waters LBFM, Trams NR, Waelkens C. 1992. A scenario for the selective depletion of stellar atmospheres. *Astron. Astrophys.* 262:L37–40
- Weaver HA, Danly L, eds. 1989. *The Formation and Evolution of Planetary Systems*. Cambridge: Univ. Press. 344 pp.
- Weissman PR. 1995. The Kuiper belt. *Annu. Rev. Astron. Astrophys.* 33:327–57
- Wetherill GW. 1990. Formation of the Earth. *Annu. Rev. Earth Planet. Sci.* 18:205–56
- Whitmire DP, Matese JJ, Whitman PG. 1992. Velocity streaming of IRAS main-sequence disk stars and the episodic enhancement of particulate disks by interstellar clouds. *Astrophys. J.* 388:190–95
- Wolstencroft RD, Scarrott SM, Gledhill TM. 1995. Properties of the  $\beta$  Pictoris disk deduced from optical imaging polarimetry. *Astroph. Space Sci.* 224:395–98
- Wolszczan A. 1994. Confirmation of Earth-mass planets orbiting the millisecond pulsar PSR B1257+12. *Science* 264:538–42
- Wolszczan A, Frail DA. 1992. A planetary system around the millisecond pulsar PSR 1257+12. *Nature* 355:145–7
- Wood J, Hashimoto A. 1993. Mineral equilibrium in fractionated nebular systems. *Geochim. Cosmochim. Acta* 57:2377–88
- Zook HA, Berg OE. 1975. A source of hyperbolic cosmic dust particles. *Planet. Space Sci.* 23:1391–97
- Zuckerman B, Becklin EE. 1993. Submillimeter studies of main-sequence stars. *Astrophys. J.* 414:793–802



## CONTENTS

THE ROLE OF STABLE ISOTOPES IN GEOCHEMISTRIES OF ALL KINDS, <i>S. Epstein</i>	1
HYDROCHEMISTRY OF FORESTED CATCHMENTS, <i>M. Robbins Church</i>	23
CHONDRULES, <i>Roger H. Hewins</i>	61
DEBRIS-FLOW MOBILIZATION FROM LANDSLIDES, <i>Richard M. Iverson, Mark E. Reid, Richard G. LaHusen</i>	85
THE EVOLUTION OF THE ALTIPLANO-PUNA PLATEAU OF THE CENTRAL ANDES, <i>Richard W. Allmendinger, Teresa E. Jordan, Suzanne M. Kay, Bryan L. Isacks</i>	139
BETA PICTORIS: An Early Solar System? <i>Pawel Artymowicz</i>	175
THERMODYNAMIC MODELS OF IGNEOUS PROCESSES, <i>Mark S. Ghiorso</i>	221
DETERMINATION OF THE COMPOSITION AND STATE OF ICY SURFACES IN THE OUTER SOLAR SYSTEM, <i>Robert H. Brown, Dale P. Cruikshank</i>	243
HYDROLOGICAL MODELING OF CONTINENTAL-SCALE BASINS, <i>Eric F. Wood, Dennis Lettenmaier, Xu Liang, Bart Nijssen, Suzanne W. Wetzel</i>	279
GPS APPLICATIONS FOR GEODYNAMICS AND EARTHQUAKE STUDIES, <i>Paul Segall, James L. Davis</i>	301
STRATIGRAPHIC RECORD OF THE EARLY MESOZOIC BREAKUP OF PANGEA IN THE LAURASIA-GONDWANA RIFT SYSTEM, <i>Paul E. Olsen</i>	337
SEDIMENT BACTERIA: Who's There, What Are They Doing, and What's New? <i>Kenneth H. Nealson</i>	403
THE ORIGIN AND EVOLUTION OF DINOSAURS, <i>Paul C. Sereno</i>	435